# CHAPTER 4

## *Synthetic seismograms and data analysis for a spherical Earth*

***4.1 Excitation of modes.*** Until now, we have been considering solutions to the homogeneous equations. We now consider the case when we have $\mathbf{f}$, an equivalent body force distribution, acting as a forcing function. Our basic equations can be written as (3.39):

$$\rho_0 \frac{\partial^2 \mathbf{s}}{\partial t^2} = \mathbf{L}(\mathbf{s}) + \mathbf{f} \tag{4.1}$$

The $k$'th free oscillation where $\mathbf{s} = \mathbf{s}_k e^{i\omega_k t}$ satisfies

$$\mathbf{L}(\mathbf{s}_k) + \rho_0 \omega_k^2 \mathbf{s}_k = 0 \tag{4.2}$$

These solutions are orthogonal and normalized such that

$$\int_V \rho_0 \mathbf{s}_{k'}^\star \mathbf{s}_k \, dV = \delta_{kk'} \tag{4.3}$$

Because of the completeness of the eigenfunctions of a self-adjoint operator, we can look for solutions to 4.1 of the form

$$\mathbf{s} = \sum_k a_k(t) \mathbf{s}_k(\mathbf{r}) \tag{4.4}$$

Substitution in 4.1 gives

$$\rho_0 \sum_k \frac{\partial^2 a_k}{\partial t^2} \mathbf{s}_k = \sum_k a_k(t) \mathbf{L}(\mathbf{s}_k) + \mathbf{f} \tag{4.5}$$

Using 4.2 gives

$$\sum_k \left[ \rho_0 \omega_k^2 a_k(t) \mathbf{s}_k + \rho_0 \frac{\partial^2 a_k}{\partial t^2} \mathbf{s}_k \right] = \mathbf{f} \tag{4.6}$$

To isolate a single $a_k(t)$, we multiply through by $\mathbf{s}_k^\star$ and integrate over the volume of the Earth. Using 4.3 then gives

$$\omega_k^2 a_k(t) + \frac{\partial^2 a_k}{\partial t^2} = \int_V \mathbf{s}_k^\star \cdot \mathbf{f}(t) \, dV = F_k(t) \quad \text{say} \tag{4.7}$$

We anticipate that $\mathbf{f}$ will be confined to a small volume around the source so $F_k(t)$ is really the result of a localized integral over the source region. The solution to 4.7 is

$$a_k(t) = \frac{1}{\omega_k} \int_{-\infty}^{t} \sin\left[\omega_k (t - t')\right] F_k(t') \, dt' \tag{4.8}$$

Equation 4.8 is not in its most useful form because an earthquake source has a body force density which is not localized in time – in fact the behavior must be nearly step-like:

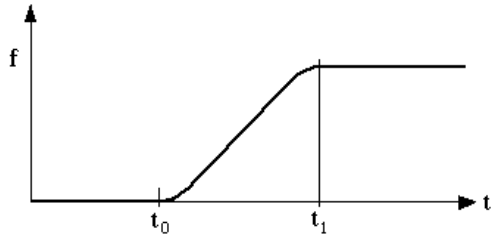


$t_0$ is the origin time of the event and $t_1 - t_0$ gives the event duration. Note that $\partial \mathbf{f}/\partial t$ is localized in time which leads us to integrate 4.8 by parts. Re-write 4.8 as

$$\begin{aligned} a_k(t) &= -\frac{1}{\omega_k^2} \int_{-\infty}^{t} \frac{d}{dt'}[1 - \cos(\omega_k(t-t'))] F_k(t')\, dt' \\ &= \frac{1}{\omega_k^2} \int_{-\infty}^{\infty} [1 - \cos(\omega_k(t-t'))] \frac{\partial}{\partial t} F_k(t')\, dt' \end{aligned} \tag{4.9}$$

We now assume that the motion is zero before t=0 and define

$$C_k(t) = [1 - \cos(\omega_k t)] H(t) \tag{4.10}$$

(where $H(t)$ is the Heaviside step function) then

$$\begin{aligned} a_k(t) &= \frac{1}{\omega_k^2} \int_{-\infty}^{\infty} C_k(t-t') \frac{\partial}{\partial t} F_k(t')\, dt' \\ &= \frac{1}{\omega_k^2} C_k(t) * \frac{\partial}{\partial t} F_k(t) \end{aligned} \tag{4.11}$$

Our formal solution to 4.1 can now be written

$$\mathbf{s}(\mathbf{r}, \mathbf{r}_0, t) = \sum_k \frac{1}{\omega_k^2} \mathbf{s}_k(\mathbf{r}) \frac{\partial}{\partial t} F_k(\mathbf{r}_0, t) * C_k(t) \tag{4.12}$$

where $\mathbf{r}$ is the receiver location and $\mathbf{r}_0$ is the source location. That is,

$$\frac{\partial F_k}{\partial t} = \int_{V_S} \mathbf{s}_k^\star \cdot \frac{\partial \mathbf{f}}{\partial t}\, dV \tag{4.13}$$

where $V_S$ is defined by the region in which $\mathbf{f}$ is non-zero. The sum in 4.12 is taken over all modes but, because we are interested only in a finite frequency band, we need include only those modes with frequencies ($\omega_k$) within that band.

Our remaining task is to evaluate 4.13 for a particular model of the seismic source. We begin with a rather general discussion of phenomenological descriptions of seismic sources. By this we mean that we shall not try to model all the complicated processes which occur during the earthquake rupture but we shall try and find an equivalent representation which accurately models the low-frequency radiation of the source.

***4.2 Moment tensors .*** The exact equations of motion in the presence of a gravitational field are:

$$\left.\begin{aligned} \rho\frac{D^2\mathbf{s}}{Dt^2} &= \nabla\cdot\mathbf{S} - \rho\nabla\phi \\ \text{and}\quad \nabla^2\phi &= 4\pi G\rho \end{aligned}\right\} \tag{4.14}$$

where $\mathbf{S}$ is the true physical stress tensor. Equations 4.14 are physical laws and are true everywhere. Up to this point, we have been considering approximate solutions to 4.14, *i.e.*, we have assumed that we have small oscillations and a linear (elastic) constitutive relationship. We anticipate that these approximations will not be valid everywhere and identify the *source region* as the place where our approximations fail. We then define the difference between our model tensor, $\mathbf{T}$, and the true physical stress, $\mathbf{S}$, as $\Gamma$ – the *stress glut*:

$$\mathbf{S} = \mathbf{T} - \Gamma \tag{4.15}$$

Comparison with 2.33 gives an expression for the equivalent body force in terms of $\Gamma$:

$$\mathbf{f} = -\nabla\cdot\Gamma \tag{4.16}$$

Thus $\mathbf{f}$ is the negative of the divergence of a second order symmetric tensor (because both $\mathbf{S}$ and $\mathbf{T}$ are symmetric). For simplicity, we shall assume that no discontinuity intersects the source region. We can then use Gauss' theorem in its simple form and show

$$\int_{V_S}\mathbf{f}\,dV = -\int_{V_S}\nabla\cdot\Gamma\,dV = -\int_{S}\Gamma\cdot\hat{\mathbf{n}}\,dS = 0 \tag{4.17}$$

(because $\Gamma$ is zero on the boundary of the source region). This result shows that no net force is applied to the Earth. Because of the symmetry of $\Gamma$, we can also show that the source exerts no net torque *i.e.*,

$$\int_{V_S}\mathbf{x}\times\mathbf{f}\,dV = 0$$

We now define the *seismic moment tensor*, $M_{ij}$ as

$$M_{ij}(t) = \int_{V_S}\Gamma_{ij}\,dV \tag{4.18}$$

so that, for a point source, $M_{ij} = \Gamma_{ij}$.

To make the algebra a little simpler, we define a local Cartesian coordinate system with $x_1 \equiv r$ (up), $x_2 \equiv \theta$ (south) and $x_3 \equiv \phi$ (east). It is then easy to show that

$$M_{ij} = \int_{V_S}x_i f_j\,dV = \int_{V_S}\Gamma_{ij}\,dV \tag{4.19}$$

Finally, we note that a point dislocation (the *double couple*) can be written in terms of the moment tensor *i.e.*,

$$M_{ij} = M_0(n_i s_j + s_i n_j) \tag{4.20}$$

where $\mathbf{n}$ is the normal to the fault plane and $\mathbf{s}$ is the *slip vector*. The double couple is the most common model for an earthquake source and our conventions describing $\mathbf{n}$ and $\mathbf{s}$ (the orientation of rupture) are described in the next section.

We now return to the evaluation of 4.13. We have to perform an integral over the source region and we suppose that the wavelengths of the modes being excited are much larger than the source dimension. If we also restrict attention to the case where there are no discontinuities intersecting the source region, we can expand $\mathbf{s}_k^\star$ in a Taylor series centered about a fiducial point, $\mathbf{x}_0$, within the source region. Thus (dropping the mode index, $k$)

$$s_j^\star = s_j^\star(\mathbf{x}_0) + (x_i - x_{0_i})\frac{\partial s_j^\star}{\partial x_i}(\mathbf{x}_0) + \frac{(x_i - x_{0_i})(x_l - x_{0_l})}{2!}\frac{\partial^2 s_j^\star}{\partial x_i \partial x_l}(\mathbf{x}_0) + \cdots \tag{4.21}$$

Substitution into 4.13 and using 4.17 gives

$$\begin{aligned}\frac{\partial F_k}{\partial t} =& \frac{\partial s_i^\star}{\partial x_j}(\mathbf{x}_0)\int\limits_{V_s} x_j \frac{\partial f_i}{\partial t}\, dV \\ &+ \tfrac{1}{2}\,\frac{\partial^2 s_i^\star}{\partial x_k \partial x_l}(\mathbf{x}_0)\left[\int\limits_{V_s} x_k x_l \frac{\partial f_i}{\partial t}\, dV - x_{0k}\int\limits_{V_s} x_l \frac{\partial f_i}{\partial t}\, dV - x_{0l}\int\limits_{V_s} x_k \frac{\partial f_i}{\partial t}\, dV\right] + \cdots\end{aligned} \tag{4.22}$$

Now let

$$\frac{\partial M_{ikl}}{\partial t} = \int\limits_{V_s} x_k x_l \frac{\partial f_i}{\partial t}\, dV = \frac{\partial M_{ilk}}{\partial t} \tag{4.23}$$

then with 4.19 we have

$$\frac{\partial F_k}{\partial t} = \frac{\partial s_i^\star}{\partial x_j}(\mathbf{x}_0)\frac{\partial M_{ij}}{\partial t} + \tfrac{1}{2}\,\frac{\partial^2 s_i^\star}{\partial x_k \partial x_l}(\mathbf{x}_0)\left[\frac{\partial M_{ikl}}{\partial t} - x_{0k}\frac{\partial M_{il}}{\partial t} - x_{0l}\frac{\partial M_{ik}}{\partial t}\right] + \cdots \tag{4.24}$$

Often, we need only retain the first term in 4.24. Remember that the origin of our coordinate system can be taken to be within the source region and we could easily let $\mathbf{x}_0$ be the origin. It is then easy to see that the second term in 4.24 will vanish as the source volume tends to zero. Then (using a dot for time derivative)

$$\begin{aligned}\frac{\partial F_k}{\partial t} \simeq& \frac{\partial s_i^\star}{\partial x_j}\frac{\partial M_{ij}}{\partial t} \qquad \text{(point source)} \\ =& \frac{\partial s_1^\star}{\partial x_1}\dot{M}_{11} + \frac{\partial s_2^\star}{\partial x_2}\dot{M}_{22} + \frac{\partial s_3^\star}{\partial x_3}\dot{M}_{33} + \left(\frac{\partial s_1^\star}{\partial x_2} + \frac{\partial s_2^\star}{\partial x_1}\right)\dot{M}_{12} \\ &+ \left(\frac{\partial s_1^\star}{\partial x_3} + \frac{\partial s_3^\star}{\partial x_1}\right)\dot{M}_{13} + \left(\frac{\partial s_2^\star}{\partial x_3} + \frac{\partial s_3^\star}{\partial x_2}\right)\dot{M}_{23} \\ =& \epsilon_{11}^\star \dot{M}_{11} + \epsilon_{22}^\star \dot{M}_{22} + \epsilon_{33}^\star \dot{M}_{33} + 2\epsilon_{12}^\star \dot{M}_{12} + 2\epsilon_{13}^\star \dot{M}_{13} + 2\epsilon_{23}^\star \dot{M}_{23}\end{aligned}$$

Thus

$$\dot{F}_k = \epsilon_k^\star : \dot{M} \tag{4.25}$$

where $\epsilon_k$ is the strain tensor of the $k$th mode evaluated at the source location. Equation 4.25 is easier to manipulate if we write out the double dot.
Let

$$\left.\begin{array}{ll} \psi_1 = \dot{M}_{11} = \dot{M}_{rr} & e_1 = \epsilon_{11} \\ \psi_2 = \dot{M}_{22} = \dot{M}_{\theta\theta} & e_2 = \epsilon_{22} \\ \psi_3 = \dot{M}_{33} = \dot{M}_{\phi\phi} & e_3 = \epsilon_{33} \\ \psi_4 = \dot{M}_{12} = \dot{M}_{r\theta} & e_4 = 2\epsilon_{12} \\ \psi_5 = \dot{M}_{13} = \dot{M}_{r\phi} & e_5 = 2\epsilon_{13} \\ \psi_6 = \dot{M}_{23} = \dot{M}_{\theta\phi} & e_6 = 2\epsilon_{23} \end{array}\right\} \tag{4.26}$$

then

$$\dot{F}_k = \sum_{i=1}^{6} e^{\star}_{ki}\psi_i \tag{4.27}$$

Thus, for a point source, 4.12 becomes

$$\mathbf{s}(\mathbf{r}, \mathbf{r}_0, t) = \sum_k \frac{1}{\omega_k^2} s_k(\mathbf{r}) \left[\sum_{i=1}^{6} e^{\star}_{ki}(\mathbf{r}_0)\psi_i\right] \star C_k(t) \tag{4.28}$$

and our source is represented by the six numbers, $\psi_i$, which in general are functions of time. Note that, if the duration of the event is small, the moment tensor will have a step function behavior so the $\psi_i(t)$ will be $\delta$-functions. The convolution in 4.28 can then be replaced by a product.

Equation 4.28 is our basic result and allows us to model seismic data at long periods (for even quite large events). For the largest events, we need more terms in the Taylor series expansion for $s^{\star}_k$. Indeed, if our fiducial point, $x_0$, is not the true location of the source, we can also generate an apparently complicated radiation pattern and equation 4.21 may not converge quickly. It is sometimes useful to vary the source location so that higher order terms are minimized. For example, if we write

$$\dot{F}_k = \frac{\partial s^{\star}_i}{\partial x_j}\dot{M}_{ij} + \tfrac{1}{2}\frac{\partial^2 s^{\star}_i}{\partial x_k \partial x_l}\dot{\tilde{M}}_{ikl} \tag{4.29}$$

where

$$\dot{\tilde{M}}_{ikl} = \frac{\partial M_{ilk}}{\partial t} - x_{0k}\frac{\partial M_{il}}{\partial t} - x_{0l}\frac{\partial M_{ik}}{\partial t}$$

then we might vary $x_0$ until the two-norm of $\dot{\tilde{M}}_{ikl}$ is minimized. The resulting value of $x_0$ which minimizes $||\dot{\tilde{M}}_{ijk}\dot{\tilde{M}}_{ijk}||$ is sometimes called the centroid location, [cf Dziewonski *et al.*, (1981) JGR, v86, p.2825].

***Problem 4.1*** Suppose you have estimated $\dot{M}_{ikl}$ and $\dot{M}_{il}$ from some seismic recordings for a particular value of $x_0$. Make an estimate of the centroid location which minimizes the two norm of $\dot{\tilde{M}}_{ijk}$. Compare your answer with the result given in the appendix of the Dziewonski *et al.*, ,1981 paper.

The procedure for finding a "centroid" location often moves an earthquake from the known location (e.g., as determined by surface faulting). Part of this may be due to the fact that low-frequency data "see" an average location of the whole rupture while a body-wave location (such as in the P.D.E.) is determined by the location of the onset of rupture. Another problem is that 3-D structure will map into the relocation and can also be confused with finite rupture propagation effects.

The moment tensor expansion technique of representing $\dot{F}_k$ becomes inefficient if we need many terms in the expansion. $M_{ij}$ has 6 independent elements but $M_{ijk}$ has 18 and $M_{ijkl}$ has 30. The total number of unknowns specifying the mode excitation goes from 6 to 24 to 54. An alternative procedure is to specify a particular kind of rupture (e.g., a propagating line rupture) and calculate the moment tensors in terms of a few parameters specifying the rupture (e.g., rupture orientation and velocity). Backus 1977a,b [GJRAS, v51, p. 1–46] gives a thorough discussion of this.

***4.3 Moment tensors and double couples .*** We work with a local cartesian coordinate system centered about a point in the source volume. We use $x_1 \equiv r$ (up), $x_2 \equiv \theta$ (South), and $x_3 \equiv \phi$ (East). Suppose we have a double-couple oriented in the 1-2 plane:

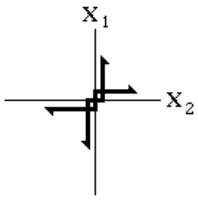


The moment tensor for this source looks like

$$M_{ij} = \begin{bmatrix} 0 & M_{12} & 0 \\ M_{21} & 0 & 0 \\ 0 & 0 & 0 \end{bmatrix}$$

where $M_{12} = M_{21} = M_0$ say. The eigenvalues of $M_{ij}$ are $\pm M_0$ and 0. Generally, the double-couple will not be aligned with our coordinate system but if we rotate the source with a rotation matrix, we will not change the eigenvalues of the moment tensor. The orientation of a double-couple is specified by the orientation of the fault plane and the motion of one wall of the fault with respect to the other (the "slip" direction). The fault orientation is traditionally specified by the fault strike ($\sigma$), dip ($\delta$) and slip ($\gamma$) angles. We can also specify it by the normal to the fault plane $(\hat{\mathbf{n}})$ and a unit vector in the direction of slip $\hat{\mathbf{s}}$). If there is no gapping or interpenetration then

$$\hat{\mathbf{n}} \cdot \hat{\mathbf{s}} = 0$$

Consider the diagram below.

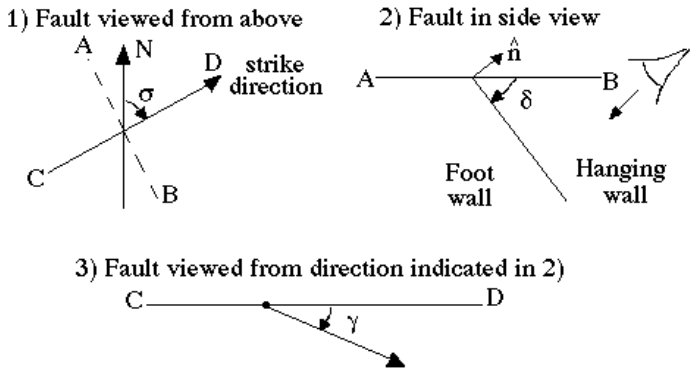


The angle between North and the trace of the fault on a horizontal surface is called the strike. The usual convention is that strike is measured positively clockwise from North with the fault dipping to the right. The dip of the fault is the angle the fault plane makes with a horizontal plane. This is measured positively down from the horizontal. A vertical fault plane has a dip of 90°. The slip of the fault has various conventions. It represents the motion of the hanging wall (the one on top) with respect to the foot wall (the one on the bottom) and is measured in the fault plane. One convention is to measure the slip direction clockwise from the horizontal strike direction. A normal fault then has a slip of 90°, a thrust fault has a slip of 270° and strike slip faults have slips of 0° or 180°. (Aki and Richards use the complement of our definition of slip, $360 - \gamma$, for the slip angle and this is now commonly used in CMT solutions. Thus a slip of 90° is a thrust fault in this convention.)

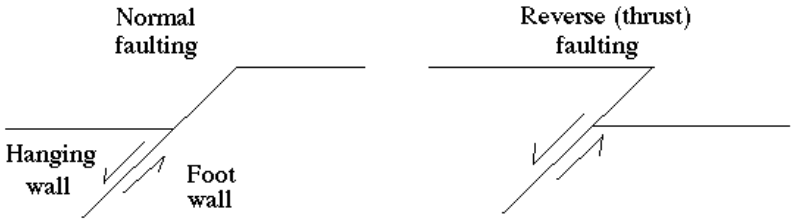


A little geometry gives

$$\begin{aligned}
\hat{n}_1 &= \cos\delta \\
\hat{n}_2 &= \sin\delta\sin\sigma \\
\hat{n}_3 &= \sin\delta\cos\sigma
\end{aligned}$$

We can also write $\hat{\mathbf{s}}$ in terms of the strike, dip and slip:

$$\begin{aligned}
\hat{s}_1 &= -\sin\gamma\sin\delta \\
\hat{s}_2 &= -\cos\gamma\cos\sigma + \sin\gamma\cos\delta\sin\sigma \\
\hat{s}_3 &= \cos\gamma\sin\sigma + \sin\gamma\cos\delta\cos\sigma
\end{aligned}$$

The equivalent force system for a double-couple is such that one force couple is oriented in the $\hat{\mathbf{n}}$ direction with the "moment arm" perpendicular to this in the $\hat{\mathbf{s}}$ direction. The other couple is oriented in the $\hat{\mathbf{s}}$ direction with its moment arm in the $\hat{\mathbf{n}}$ direction. As far as the radiation pattern is concerned,

we can interchange $\hat{\mathbf{n}}$ and $\hat{\mathbf{s}}$ (or equivalently, the fault plane and auxilliary plane) with no change in the observed waveforms). Thus

$$M_{ij} = M_0(n_i s_j + s_i n_j)$$

gives the moment tensor elements equivalent to a double-couple.

Note that a double-couple requires four numbers ($M_0, \sigma, \delta, \gamma$) to describe it whereas a general moment tensor has six independent numbers (remember that it is symmetric). We can therefore specify a more complicated source than a double-couple with the moment tensor. If the moment tensor is trace-free ($M_{11} + M_{22} + M_{33} = 0$) as it is for a double-couple, it means that the radiation pattern has no isotropic component as would be generated by an explosive or implosive source. Natural sources do not seem to have a significant isotropic component so the condition that the moment tensor is trace-free is often imposed "a priori". This reduces the number of independent moment tensor elements to five (which is still more than that needed for a double-couple).

As we shall see, it is more convenient to solve for the five elements of $\mathbf{M}$ in a linear problem than to solve the non-linear problem for $M_0, \sigma, \delta$ and $\gamma$ which specify the double-couple. The resulting moment tensor can be decomposed in a variety of ways. A convenient way of visualising the moment tensor solution is to decompose it into a 'major double-couple" and a "minor double-couple". If the moment tensor is already a double-couple, it has eigenvalues $(\lambda, 0, -\lambda)$. Generally this will not be true and we work with the trace-free (deviatoric) part of $\mathbf{M}$:

$$M_{ij} = \frac{1}{3} M_{kk} \delta_{ij} + D_{ij}$$

where, by construction, $\mathbf{D}$ is trace-free. We now decompose $\mathbf{D}$ into its eigenvalues and eigenvectors:

$$\mathbf{D} = \mathbf{U} \mathbf{\Lambda} \mathbf{U}^T$$

where $\mathbf{\Lambda}$ is a diagonal matrix of eigenvalues with

$$\mathbf{\Lambda} = (\lambda_1, \lambda_2, \lambda_3)$$

$$\text{and} \quad |\lambda_1| > |\lambda_2| > |\lambda_3|$$

$$\text{and} \quad \lambda_1 + \lambda_2 + \lambda_3 = 0$$

This last relationship follows because the trace of $\mathbf{D}$ is equal to the trace of $\mathbf{\Lambda}$. Now let

$$\mathbf{\Lambda}_1 = (\lambda_1, -\lambda_1, 0) \quad \text{and} \quad \mathbf{\Lambda}_3 = (0, -\lambda_3, \lambda_3)$$

so that $\mathbf{\Lambda} = \mathbf{\Lambda}_1 + \mathbf{\Lambda}_3$ and both $\mathbf{\Lambda}_1$ and $\mathbf{\Lambda}_3$ have the forms of double-couples. $\mathbf{D}$ can now be written

$$\mathbf{D} = \mathbf{U} \mathbf{\Lambda}_1 \mathbf{U}^T + \mathbf{U} \mathbf{\Lambda}_3 \mathbf{U}^T$$

where the first term on the right is the major double-couple and the second term is the minor double-couple. In nearly all cases, the major double-couple is a factor of ten or more greater than the minor double-couple. If they are of similar magnitude, it is usually because the event is a multiple event (not a point source) or some blunder in the data handling has occurred.

The final step is to go from the eigenvalue/eigenvector decomposition of a double-couple to a description in terms of strike, dip and slip. We write out the explicit form of the moment tensor, $\mathbf{U} \mathbf{\Lambda} \mathbf{U}^T$, for

either double-couple and compare with the expression in terms $M_0$, $\hat{\mathbf{n}}$ and $\hat{\mathbf{s}}$. Now $\lambda_2 = -\lambda_1 = -M_0$ and $\lambda_3 = 0$ and let $\mathbf{u}^1$ be the eigenvector associated with $\lambda_1$ and $\mathbf{u}^2$ be the eigenvector associated with $\lambda_2$. We then obtain

$$\hat{\mathbf{n}} = \frac{1}{\sqrt{2}}(\mathbf{u}^1 + \mathbf{u}^2)$$

$$\hat{\mathbf{s}} = \frac{1}{\sqrt{2}}(\mathbf{u}^1 - \mathbf{u}^2)$$

The right hand sides of these equation can be interchanged and the signs of both $\hat{\mathbf{n}}$ and $\hat{\mathbf{s}}$ can be flipped. We fix the sign by using the convention that dip $(\delta)$ lies between 0° and 90°. The relation $\hat{n}_1 = \cos\delta$ therefore means that $\hat{n}_1$ must be taken as positive. From the definitions of $\hat{\mathbf{n}}$ and $\hat{\mathbf{s}}$, we obtain

$$\tan\delta = \frac{\sqrt{1-\hat{n}_1^2}}{\hat{n}_1}$$

$$\tan\sigma = \frac{\hat{n}_2}{\hat{n}_3}$$

$$\tan\gamma = \frac{-\hat{s}_1}{\hat{s}_3\hat{n}_2 - \hat{s}_2\hat{n}_3}$$

Interchanging the expressions for $\hat{\mathbf{n}}$ and $\hat{\mathbf{s}}$ gives us first the strike, dip and slip of the fault plane and then the strike, dip and slip of the auxilliary plane. Of course, we can't distinguish between the fault and auxilliary planes unless we have additional information.

Sometimes we will have some information about the orientation of one of the planes of the double-couple. This information would typically be the strike and dip of the fault plane deduced from the local tectonics, or the strike and dip of one plane constrained by a fault plane solution. Given this information, we can compute $\hat{\mathbf{n}}$ and then write

$$\boldsymbol{\psi} = \begin{bmatrix} 2\hat{n}_1 & 0 & 0 \\ 0 & 2\hat{n}_2 & 0 \\ 0 & 0 & 2\hat{n}_3 \\ \hat{n}_2 & \hat{n}_1 & 0 \\ \hat{n}_3 & 0 & \hat{n}_1 \\ 0 & \hat{n}_3 & \hat{n}_2 \end{bmatrix} \begin{bmatrix} -\sin\delta & 0 \\ \cos\delta\sin\sigma & -\cos\sigma \\ \cos\delta\cos\sigma & \sin\sigma \end{bmatrix} \begin{bmatrix} M_0\sin\gamma \\ M_0\cos\gamma \end{bmatrix}$$

or

$$\boldsymbol{\psi} = \mathbf{N}\cdot\mathbf{x}$$

where $\mathbf{x} = (M_0\sin\gamma, M_0\cos\gamma)$ and $\boldsymbol{\psi}$ is the vector of the six elements of the moment tensor (see equation 4.26 below). $\mathbf{N}$ can be computed so $\boldsymbol{\psi}$ is now linearly related to $\mathbf{x}$ which can therefore be found by linear inversion of seismic data in the same way we solve for $\boldsymbol{\psi}$ below. From $\mathbf{x}$, we obtain $M_0$ and $\gamma$:

$$M_0 = |\mathbf{x}| \quad \text{and} \quad \tan\gamma = \frac{x_1}{x_2}$$

which completes the double-couple solution since we are given the strike and dip.

***4.4 Greens function in epicentral coordinates .*** The evaluation of 4.28 is laborious and can be made much faster if we can assume the Earth is spherically symmetric. If this is valid, all $2l+1$ oscillations with the same $n, l$ have the same frequency (i.e., $-l \leq m \leq l$) and we can perform the sum over $m$ analytically. This is most efficiently done if we adopt an epicentral coordinate system with the epicenter at the pole. The advantage of this scheme is that $e_k$ is zero in epicentral coordinates unless $m \leq 2$.

To make the angles we are using completely clear we consider the following spherical triangle:

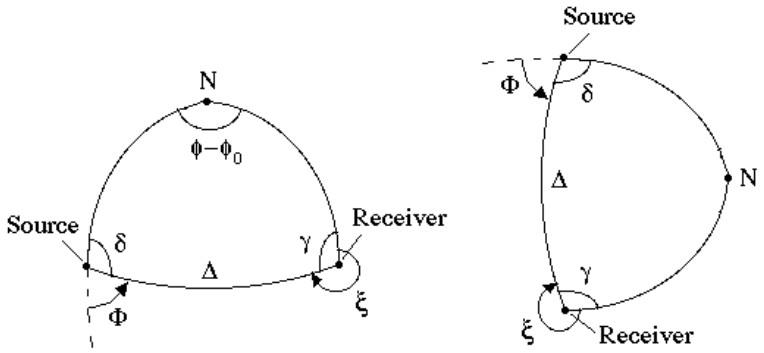


$\Delta$ is epicentral distance (colatitude), $\Phi$ is epicentral longitude, $\xi = 2\pi - \gamma$.

$$
\begin{aligned}
\cos\Delta &= \cos\theta\cos\theta_0 + \sin\theta\sin\theta_0\cos(\phi-\phi_0) \\
\sin\Delta &= (1 - \cos^2\Delta)^{\frac{1}{2}} \\
\sin\delta &= \sin\Phi = \sin(\phi-\phi_0)\sin\theta/\sin\Delta \\
\cos\delta &= -\cos\Phi = (\cos\theta - \cos\theta_0\cos\Delta)/(\sin\theta_0\sin\Delta) \\
\sin\xi &= -\sin(\phi-\phi_0)\sin\theta_0/\sin\Delta \\
\cos\xi &= (\cos\theta_0 - \cos\theta\cos\Delta)/(\sin\theta\sin\Delta)
\end{aligned}
$$

(The source is at $\theta_0, \phi_0$ and the receiver is at $\theta, \phi$). We have given formulae for $\xi$ (which is the aximuth of the source from the receiver measured clockwise from north) because we need it to rotate horizontal components. Consider the receiver

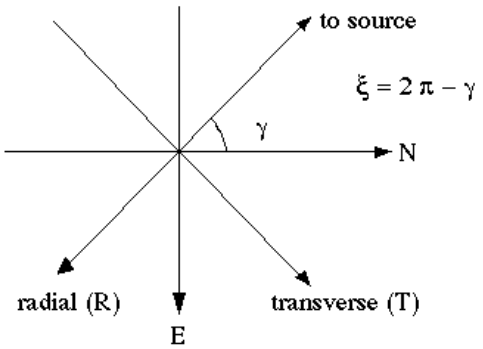


In epicentral coordinates, we shall be using radial and transverse coordinates (i.e., $\hat{\boldsymbol{\theta}}$ and $\hat{\boldsymbol{\phi}}$) but we measure North/South and East/West. A little algebra shows that

$$A_{N-S} = -\cos\xi\, A_{\hat{\boldsymbol{\theta}}} - \sin\xi\, A_{\hat{\boldsymbol{\phi}}}$$
$$A_{E-W} = -\sin\xi\, A_{\hat{\boldsymbol{\theta}}} + \cos\xi\, A_{\hat{\boldsymbol{\phi}}}$$

where $A_{\hat{\boldsymbol{\theta}}}$ and $A_{\hat{\boldsymbol{\phi}}}$ are the components of displacement in the radial and transverse direction and $A_{N-S}$, $A_{E-W}$ are the measured components.

[You sould remenber that $\theta$ in the above formulae is geocentric colatitude. Station locations, source locations, etc. are nearly always given in geographic colatitudes. The main difference arises because of the elliptical flattening of the Earth. An exaggerated sketch of the situation is given below.

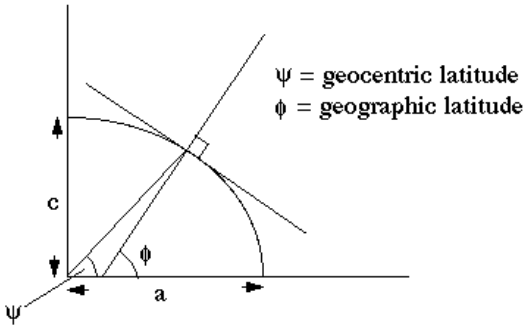


$$\tan\psi = (1-f)^2 \tan\phi$$

where $f$ is the flattening of the Earth, i.e., $f = \frac{a-c}{a} = \frac{1}{298.256}$ .]

We now rewrite equation 4.28 to make the sum over $m$ explicit:

$$\mathbf{s}(\mathbf{r}, \mathbf{r}_0, t) = \sum_{n,l} \sum_{i=1}^{6} \left[ \sum_{m=-l}^{l} {}_n\mathbf{s}_l^m(\mathbf{r})\, {}_n e_{li}^{m^\star} \right] \cdot \psi_i(t) \star \frac{1}{{}_n\omega_l^2}\, {}_nC_l(t) \tag{4.30}$$

where ${}_nC_l(t) = [1 - \cos {}_n\omega_l t]H(t)$.
Note that, for spheroidal modes

$${}_n\mathbf{s}_l^m(\mathbf{r}) = \hat{\mathbf{r}}\, {}_nU_r(r) Y_l^m(\Delta, \Phi) + {}_nV_l(r) \nabla_1 Y_l^m(\Delta, \Phi) \tag{4.31}$$

and, for toroidal modes

$${}_n\mathbf{s}_l^m(\mathbf{r}) = -\hat{\mathbf{r}} \times {}_nW_l(r) \nabla_1 Y_l^m(\Delta, \Phi) \tag{4.32}$$

The strain tensor in spherical polar coordinates is given by equation A22. It is a little tricky to find the limiting values of $\epsilon$ at the pole since there are several apparent singularities in equation A22. When $\epsilon$ is expressed in terms of generalized spherical harmonics, the value at the pole can be written down by inspection because of the property

$$Y_l^{N,m}(0,0) = \delta_{Nm}.$$

The result of taking this limit is given in Table A1. We now evaluate the sum in 4.30 for the vertical component of a spheroidal mode (the other components follow in a similar fashion). We consider each value of $i$ separately (see equation 4.26).

$i = 1$ ($rr$ component). Note that only $m = 0$ contributes.

$$\sum_{m=-l}^{l} {}_n\mathbf{s}_l^m(\mathbf{r}) {}_n e_{l1}^{m^\star}(\mathbf{r}_0) = \hat{\mathbf{r}}_n U_l(r_a) Y_l^0(\Delta) \frac{dU}{dr}(r_0) d_l^0$$
$$= \hat{\mathbf{r}}_n U_l(r_a) \frac{d_n U_l}{dr}(r_0) d_l^0 X_l^0$$

(Note $Y_l^m = X_l^m e^{im\phi}$, $Y_l^{-m} = (-1)^m Y_l^{m^\star}$, $r_a$ is the receiver radius, $r_0$ is the source radius, and $X_l^m = X_l^m(\Delta)$)

$i = 2$ ($\theta\theta$ component)

$$\sum_{m=-l}^{l} {}_n\mathbf{s}_l^m(\mathbf{r}) {}_n e_{l2}^{m^\star}(\mathbf{r}_0) = \hat{\mathbf{r}}_n U_l(r_a) \left[ \frac{F}{2} d_l^0 X_l^0 + \frac{V}{r_0} d_l^2 X_l^{-2} e^{-2i\Phi} + \frac{V}{r_0} d_l^2 X_l^2 e^{2i\Phi} \right]$$
$$= \hat{\mathbf{r}}_n U_l(r_a) \left[ \frac{F}{2} d_l^0 X_l^0 + \frac{2V}{r_0} d_l^2 X_l^2 \cos 2\Phi \right]$$

$i = 3$ ($\phi\phi$ component)

$$\sum_{m=-l}^{l} {}_n\mathbf{s}_l^m(\mathbf{r}) {}_n e_{l3}^{m^\star}(\mathbf{r}_0) = \hat{\mathbf{r}}_n U_l(r_a) \left[ \frac{F}{2} d_l^0 X_l^0 - \frac{V}{r_0} d_l^2 X_l^{-2} e^{-2i\Phi} - \frac{V}{r_0} d_l^2 X_l^2 e^{2i\Phi} \right]$$
$$= \hat{\mathbf{r}}_n U_l(r_a) \left[ \frac{F}{2} d_l^0 X_l^0 - \frac{2V}{r_0} d_l^2 X_l^2 \cos 2\Phi \right]$$

$i = 4$ ($r\theta$ component)

$$\sum_{m=-l}^{l} {}_n\mathbf{s}_l^m(\mathbf{r}) {}_n e_{l4}^{m^\star}(\mathbf{r}_0) = \hat{\mathbf{r}}_n U_l(r_a) [\mathrm{X} d_l^1 X_l^{-1} e^{-i\Phi} - \mathrm{X} d_l^1 X_l^1 e^{i\Phi}]$$
$$= \hat{\mathbf{r}}_n U_l(r_a) 2\mathrm{X} d_l^1 X_l^1 \cos\Phi$$

where $\mathrm{X} = \frac{dV}{dr} + \frac{U-V}{r}$

$i = 5$ ($r\phi$ component)

$$\sum_{m=-l}^{l} {}_n\mathbf{s}_l^m(\mathbf{r}) {}_n e_{l5}^{m^\star}(\mathbf{r}_0) = \hat{\mathbf{r}}_n U_l(r_a) [i\mathrm{X} d_l^1 X_l^{-1} e^{-i\Phi} + i\mathrm{X} d_l^1 X_l^1 e^{i\Phi}]$$
$$= \hat{\mathbf{r}}_n U_l(r_a) \mathrm{X} d_l^1 X_l^1 [-ie^{-i\Phi} + ie^{i\Phi}]$$
$$= \hat{\mathbf{r}}_n U_l(r_a) 2\mathrm{X} d_l^1 X_l^1 \sin\Phi$$

$i = 6$ ($\theta\phi$ component)

$$\sum_{m=-l}^{l} {}_n\mathbf{s}_l^m(\mathbf{r}) {}_n e_{l6}^{m^\star}(\mathbf{r}_0) = \hat{\mathbf{r}}_n U_l(r_a) \left[ \frac{2iV}{r_0} d_l^2 X_l^{-2} e^{-2i\Phi} - \frac{2iV}{r_0} d_l^2 X_l^2 e^{2i\Phi} \right]$$
$$= \hat{\mathbf{r}}_n U_l(r_a) d_l^2 X_l^2 \frac{4V}{r_0} \sin 2\Phi$$

In these formulae, $F[=(2U-l(l+1)V)/r]$, X and $V$ should all be evaluated at the source depth, $r_0$. Summarizing results for all components gives

$$ {}_n\mathbf{G}_l^i = \sum_{m=-l}^{l} {}_n\mathbf{s}_l^m(\mathbf{r}) {}_n e_{li}^{m^\star}(\mathbf{r}_0) = \hat{\mathbf{r}}\, {}_nU_l(r_a) g_i + {}_nV_l(r_a)\nabla_1 g_i - \hat{\mathbf{r}} \times {}_nW_l(r_a)\nabla_1 h_i \tag{4.33} $$

with

$$ \left.\begin{array}{cc} g_1 = \frac{dU}{dr} d_l^0 X_l^0 & h_1 = 0 \\ g_2 = \frac{F}{2} d_l^0 X_l^0 + \frac{2V}{r_0} d_l^2 X_l^2 \cos 2\Phi & h_2 = \frac{2W}{r_0} d_l^2 X_l^2 \sin 2\Phi \\ g_3 = \frac{F}{2} d_l^0 X_l^0 - \frac{2V}{r_0} d_l^2 X_l^2 \cos 2\Phi & h_3 = -\frac{2W}{r_0} d_l^2 X_l^2 \sin 2\Phi \\ g_4 = 2\mathrm{X} d_l^1 X_l^1 \cos\Phi & h_4 = 2Z d_l^1 X_l^1 \sin\Phi \\ g_5 = 2\mathrm{X} d_l^1 X_l^1 \sin\Phi & h_5 = -2Z d_l^1 X_l^1 \cos\Phi \\ g_6 = \frac{4V}{r_0} d_l^2 X_l^2 \sin 2\Phi & h_6 = -\frac{4W}{r_0} d_l^2 X_l^2 \cos 2\Phi \end{array}\right\} \tag{4.34} $$

and

$$ \mathbf{s}(\mathbf{r}, \mathbf{r}_0, t) = \sum_{n,l} \sum_{i=1}^{6} {}_n\mathbf{G}_l^i(\mathbf{r}, \mathbf{r}_0) \psi_i(t) \star \frac{1}{{}_n\omega_l^2} {}_nC_l(t) \tag{4.35} $$

Note that, given a model of the Earth, we can compute everything in this formula except for $\psi$. $\psi$ is determined by the moment tensor so we can compute synthetic seismograms given a source mechanism.

[Note that

$$ d_l^k X_l^k = \frac{1}{2^k} \left( \frac{2l+1}{4\pi} \right) P_l^k(\cos\theta) $$

and can easily be computed using the recursion over $l$ for the $P_l^k$'s (see Appendix B). This is efficient since we usually need all $l$ values up to some maximum $l$ and only a few low values of $k$ ($k \leq 2$ for a point source).]

Equation 4.35 gives us the displacement field at some measurement location, $\mathbf{r}$, but this is not what we actually measure with a seismometer. We now consider the response of a seismometer in more detail.

***4.5 Response of a seismometer .*** Most seismographs are accelerometers and one might expect that all we would have to do is to multiply 4.35 by $-\omega_k^2$ and we would have the acceleration for an oscillation of the form $\mathbf{s}_k e^{i\omega_k t}$. This is not strictly true. When there is vertical motion, the seismeter is moving in a gravity field and tilt occurs. Furthermore, the mode of oscillation itself perturbs the gravitational field and so modifies the acceleration at the recording site (this latter effect is only important at very low frequencies).

We sketch the situation as follows

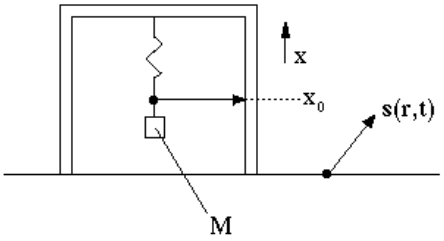


The local Earth displacement is $\mathbf{s}(\mathbf{r}, t)$. The rest position of the seismometer is $x_0$ and the mass moves an amount $x$ relative to the housing the the instrument. We measure $x$ or, in a fed-back system, the force that must be applied to $M$ to keep $M$ motionless with respect to the housing. We consider the seismometer as a damped oscillator with damping constant $\gamma$ and natural frequency $\omega_0$. Let $\hat{\mathbf{p}}$ be the polarization vector of the seismometers (e.g., $\hat{\mathbf{p}} = \hat{\mathbf{r}}$ for a vertical component instrument). The total force per unit mass acting on $M$ is given by

$$\hat{\mathbf{p}} \cdot \ddot{\mathbf{s}} + \ddot{x} + \gamma \dot{x} + \omega_0^2 (x - x_0) \equiv \hat{\mathbf{p}} \cdot \mathbf{a} \tag{4.36}$$

$\mathbf{a}$ is the "acceleration due to gravity", *i.e.*,

$$\mathbf{a} = -\nabla \phi$$

$$\phi = \phi_0 + \phi_1 + \phi_E \cdots$$

$\phi_E$ is an external tidal potential but we shall neglect this (since the tides are usually removed from the seismic recordings before processing) and consider $\phi$ as a sum of the unperturbed gravitational potential, $\phi_0$, and the perturbation in $\phi_0$ due to the motion, $\phi_1$.

Remember that $\nabla \phi_0 = \hat{\mathbf{r}} g_0(r)$, so that in the rest position when $\mathbf{s}$ and $\phi_1$ are zero we have

$$-\omega_0^2 x_0 = -\hat{\mathbf{p}}_0 \cdot \hat{\mathbf{r}} g_0(r_s) \tag{4.37}$$

and $\hat{\mathbf{p}}_0$ is the undisturbed polarization vector (remember, we shall have to worry about tilt). $r_s$ is the (undisturbed) radius of the instrument. Equation 4.36 becomes

$$\hat{\mathbf{p}} \cdot \ddot{\mathbf{s}} + \ddot{x} + \gamma \dot{x} + \omega_0^2 x = -\hat{\mathbf{p}} \cdot \hat{\mathbf{r}} g_0(r) + \hat{\mathbf{p}}_0 \cdot \hat{\mathbf{r}} g_0(r_s) - \hat{\mathbf{p}} \cdot \nabla \phi_1$$

$r$ is the instantaneous position of the housing, *i.e.*,

$$r = r_s + \hat{\mathbf{r}} \cdot \mathbf{s}$$

Now we let

$$g_0(r) \simeq g_0(r_s) + \frac{\partial g_0}{\partial r}(r_s)(\hat{\mathbf{r}} \cdot \mathbf{s})$$

so that

$$\ddot{x} + \gamma \dot{x} + \omega_0^2 x = -\hat{\mathbf{p}} \cdot \ddot{\mathbf{s}} - (\hat{\mathbf{p}} - \hat{\mathbf{p}}_0) \cdot \hat{\mathbf{r}} g_0(r_s) - \hat{\mathbf{p}} \cdot \hat{\mathbf{r}} \frac{\partial g_0}{\partial r}(r_s)(\hat{\mathbf{r}} \cdot \mathbf{s}) - \hat{\mathbf{p}} \cdot \nabla \phi_1 \tag{4.38}$$

$\hat{\mathbf{r}} \cdot \mathbf{s}$ varies laterally so there is tilting of the instrument (in general) and this then is given by $\hat{\mathbf{p}} - \hat{\mathbf{p}}_0$.

Consider equation 4.38 for a vertically polarized seismometer, *i.e.*, $\hat{\mathbf{p}} = \hat{\mathbf{r}}$ so (using equation 2.20)

$$\hat{\mathbf{p}} - \hat{\mathbf{p}}_0 = -\frac{1}{r_s}\nabla_1(\hat{\mathbf{r}} \cdot \mathbf{s})$$

and thus

$$\ddot{x} + \gamma\dot{x} + \omega_0^2 x = -\ddot{s}_r - \frac{\partial g_0}{\partial r}(r_s)s_r - \frac{\partial \phi_1}{\partial r}(r_s) \tag{4.39}$$

(Note $\nabla_1$ is perpendicular to $\hat{\mathbf{r}}$ so that the tilt term goes away.) For a horizontally polarized seismometer, we let $s_t$ denote the displacement in the $\hat{\mathbf{t}}$ direction. Then from 4.38 and 2.21

$$\ddot{x} + \gamma\dot{x} + \omega_0^2 x = -\ddot{s}_t - \frac{1}{r_s}(\hat{\mathbf{t}} \cdot \nabla_1 s_r)g_0(r_s) - \frac{\hat{\mathbf{t}}}{r_s} \cdot \nabla_1 \phi_1 \tag{4.40}$$

The right hand side of 4.39 and 4.40 is a direct measure of the force (per unit mass) on the seismometer and so is proportional to what is actually measured in a fed-back system. For a vertical component, we have (in addition to the acceleration of the Earth's surface) the effect of movement in a gravity gradient and an effect due to the redistribution of mass due to the motion. For a horizontal component we have an effect due to tilt and also an effect due to redistribution of mass.

We now consider the right hand side of 4.39 and 4.40 for a particular mode of oscillation of the Earth. Since we are on the surface of the Earth, $\phi_1$ satisfies Lapaces equation, so

$$\phi_1(r) = \phi_1(r_s)\left(\frac{r_s}{r}\right)^{l+1}$$

and also

$$\frac{dg_0}{dr}(r_s) = -\frac{2g_0}{r_s}.$$

Equation 4.39 now reads

$$-\ddot{s}_r - \frac{\partial g_0}{\partial r}(r_s)s_r - \frac{\partial \phi_1}{\partial r}(r_s) = \omega_k^2 s_r + \frac{2g_0}{r_s}s_r + \frac{l+1}{r_s}\phi_1(r_s) \tag{4.41}$$

This is valid at the surface. A buried seismometer where $\rho_0(r_s) \neq 0$ has a response like

$$\omega_k^2 s_r + \frac{2g_0(r_s)}{r_s}s_r - \left[\frac{d\phi_1}{dr} + 4\pi G\rho_0(r_s)s_r\right]$$

Inspection of 4.41 shows that, if the radial component of displacement is given by $\hat{\mathbf{r}}_n U_l(r_s)Y_l^m$ times an excitation factor, an accelerometer will measure $\hat{\mathbf{r}}_n A U_l Y_l^m$ times an excitation factor, where

$${}_nAU_l = {}_n\omega_l^2\,{}_nU_l(r_s) + \frac{2g_0(r_s)}{r_s}{}_nU_l(r_s) + \frac{l+1}{r_s}{}_n\Phi_{1l}(r_s) \tag{4.42}$$

or

$$AU = AU_1 + AU_2 + AU_3 \quad \text{say}$$

Here is a table of values:

| mode | $AU_1/AU$ | $AU_2/AU$ | $AU_3/AU$ | $\omega$ mHz |
|---|---|---|---|---|
| ${}_0S_2$ | .815 | .667 | -.482 | .309 |
| ${}_0S_{10}$ | .983 | .025 | -.008 | 1.726 |
| ${}_8S_1$ | .991 | .009 | – | 2.871 |

It is only at very low frequencies that we make a significant error if we neglect $AU_2$ and $AU_3$.

For the horizontal component of a spheroidal mode, the displacement is proportional to ${}_nV_l(r_s)\hat{\mathbf{t}} \cdot \nabla_1 Y_l^m$ and the right hand side of 4.40 can be written

$$\hat{\mathbf{t}} \cdot [\omega_k^2 \mathbf{s} - \frac{1}{r_s}\nabla_1 s_r g_0(r_s) - \frac{1}{r_s}\nabla_1 \phi_1]$$

$$= \hat{\mathbf{t}} \cdot [\omega_{kn}^2 V_l - \frac{{}_nU_l}{r_s} g_0 - \frac{1}{r_s}{}_n\Phi_{1l}]\nabla_1 Y_l^m$$

so that we measure on acceleration times an excitation vector where the acceleration scalar, ${}_nAV_l$, is given by

$${}_nAV_l = \omega_{kn}^2 V_l - \frac{{}_nU_l}{r_s} g_0 - \frac{1}{r_s}{}_n\Phi_{1l} \tag{4.43}$$

or

$$AV = AV_1 + AV_2 + AV_3$$

A table of values:

| mode | $AV_1/AV$ | $AV_2/AV$ | $AV_3/AV$ | $\omega$ mHz |
|---|---|---|---|---|
| ${}_0S_2$ | -.118 | 2.133 | -1.015 | .309 |
| ${}_0S_{10}$ | .868 | .140 | -.008 | 1.726 |
| ${}_8S_1$ | 1.045 | -.045 | – | 2.871 |

Note the relatively drastic effect of tilt on the measured acceleration of ${}_0S_2$ – this is largely because the frequency is so low that the $AV_2$ and $AV_3$ become relatively more important.

Finally we note that a toroidal mode has no vertical motion and no tilting and does not disturb the gravitational field. The acceleration scalar for a toroidal mode is therefore

$$AW =_n \omega_l^2 {}_nW_l(r_s)$$

***4.6 Source retrieval .*** When we measure acceleration, 4.35 becomes

$$\mathbf{a}(\mathbf{r}, \mathbf{r}_0, t) = \sum_{n,l}\sum_{i=1}^{6} {}_n\mathbf{G}_l^i(\mathbf{r}, \mathbf{r}_0)\psi_i(t) \star \frac{1}{{}_n\omega_l^2}{}_nC_l(t) \tag{4.44}$$

where (4.32) now becomes modified to read

$${}_n\mathbf{G}_l^i = \hat{\mathbf{r}}\,{}_nAU_l(r_a)g_i + {}_nAV_l(r_a)\nabla_1 g_i - \hat{\mathbf{r}} \times {}_nAW_l(r_a)\nabla_1 h_i$$

Before we can use 4.44 to model real data, we must include the effect of attenuation. We calculate this effect using perturbation theory. From chapter 2, we found that a linear viscoelastic medium with weak, nearly frequency independent attenuation has "elastic" moduli which can be written, e.g.,

$$\mu(\omega) = \mu_0(\omega_r)\left[1 + \frac{2}{\pi Q_\mu}\ln\left(\frac{\omega}{\omega_r}\right) + \frac{i}{Q_\mu}\right]$$

where $\omega_r$ is a reference frequency. We are currently interested in the small imaginary perturbation, *i.e.*,

$$\mu \to \mu + \delta\mu \quad \text{where} \quad \delta\mu = \frac{i\mu_0}{Q_\mu} \tag{4.45}$$

As we shall show in later sections, this results in a perturbation to the squared frequency of the mode, *i.e.*,

$$\omega_k^2 \to \omega_k^2 + \delta(\omega_k^2)$$

In this case, $\delta(\omega_k^2)$ is purely imaginary, so by analogy with 4.45, we write

$$\frac{\delta(\omega_k^2)}{\omega_k^2} = \frac{i}{Q_k}$$

where $Q_k$ is the $Q$ of the $k$th mode. We rearrange this to give

$$\delta\omega_k = \frac{i\omega_k}{2Q_k} = i\alpha_k$$

so

$$\omega_k \to \omega_k + i\alpha_k \quad \text{with} \quad \alpha_k = \frac{\omega_k}{2Q_k} \tag{4.46}$$

Later on, we shall see how to compute $Q_k$ given $Q_\mu$ as a function of depth (and frequency) inside the Earth. For now, we assume this has been done so that any oscillatory motion, $e^{i\omega_k t}$, now acquires an exponetial decay factor, $e^{-\alpha_k t}$. Equation 4.44 can now be modified to include this by modifying ${}_nC_l(t)$ so that

$${}_nC_l(t) = [1 - \cos({}_n\omega_l t)e^{-{}_n\alpha_l t}]H(t) \tag{4.47}$$

Suppose we are given a model of the Earth. Inspection of 4.44 shows that we can calculate everything but $\psi_i(t)$ – the source mechanism.
Define

$$\mathbf{B}_i(\mathbf{r}, \mathbf{r}_0, t) = \sum_{n,l} \frac{1}{{}_n\omega_l^2}\,{}_n\mathbf{G}_l^i(\mathbf{r}, \mathbf{r}_0)\,{}_nC_l(t) \tag{4.48}$$

so equation 4.44 reads

$$\mathbf{a}(\mathbf{r}, \mathbf{r}_0, t) = \sum_{i=1}^{6} \mathbf{B}_i(\mathbf{r}, \mathbf{r}_0, t) \star \psi_i(t) \tag{4.49}$$

If we now denote a single component of recording for the $(\mathbf{r}, \mathbf{r}_0)$ source-receiver pair by the index $j$ and Fourier transform 4.49, we obtain

$$a_j(\omega) = \sum_{i=1}^{6} B_{ij}(\omega)\psi_i(\omega) \tag{4.50}$$

which is a parameter-estimation problem for the unknown vector $\psi_i$. Note that if $\psi_i(t)$ is $\delta$-like in time then $\psi_i$ will be nearly independent of frequency. In practice, we often assume that all elements of $\psi_i$ have the same time dependence, *i.e.*,

$$\psi_i(t) = \psi_i s(t) \tag{4.51}$$

Furthermore, the exact shape of $s(t)$ has only a weak effect on the shape of the long-period spectrum. We usually use a triangle function

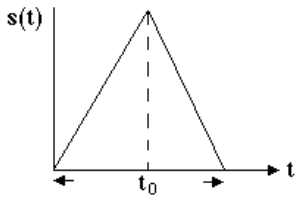


The triangle is the convolution of a boxcar of length $t_0/2$ with itself and the spectrum of a boxcar is just

$$\begin{aligned}
\int_0^{t_0/2} e^{-i\omega t}\, dt &= \left[-\frac{1}{i\omega} e^{-i\omega t}\right]_0^{t_0/2} = \frac{1}{i\omega} - \frac{1}{i\omega} e^{-i\omega t_0/2} \\
&= \frac{2e^{-i\omega t_0/4}}{2i\omega}[e^{i\omega t_0/4} - e^{-i\omega t_0/4}] \\
&= \frac{2e^{-i\omega t_0/4}}{\omega} \sin\frac{\omega t_0}{4} = \frac{t_0}{2} e^{-i\omega t_0/4} \,\mathrm{sinc}\,(\frac{\omega t_0}{4})
\end{aligned}$$

The spectrum of a triangle function is just the square of this, *i.e.*,

$$s(\omega) = \frac{t_0^2}{4} e^{-i\omega t_0/2} \,\mathrm{sinc}^{\,2}(\frac{\omega t_0}{4}) \tag{4.52}$$

The important factor in 4.52 is the apparent origin shift of $e^{-i\omega t_0/2}$ (the $\mathrm{sinc}^{\,2}$ term is very slowly varying at low frequencies for all but the largest events). This effect can sometimes be seen in the data for big events if a body-wave determined origin time is used in the calculations. The low frequency energy "sees" a later time than the body waves as the relevant periods are longer than the rupture time and so see an average of the whole rupture. In contrast, the $P$-wave origin time corresponds to the onset of rupture.

One way to proceed is to make a guess of $t_0$, compute $s(\omega)$ then include this effect in $B_{ij}(\omega)$. We may then solve 4.50 for 6 frequency-independent numbers. $t_0$ may be varied until the best fit to the data is achieved.

A reasonable question is: How much information do we need to be able to solve 4.50 for $\psi_i$? If $\psi_i$ is frequency independent then it might be thought that we only need six extimates of $a(\omega)$ at a single recording for six different frequencies to get a solution. This is not quite true. Inspection of 4.34 shows that, for a particular station, $g_i$ is made up of a linear combination of four functions: $(\frac{dU}{dr} d_l^0 X_l^0$, $\frac{F}{2} d_l^0 X_l^0$, $\frac{V}{r_0} d_l^2 X_l^2$, X$d_l^1 X_l^1)$ so that $B_{ij}$ will be rank deficient if we have only one recording. This deficiency will be formally removed if we have two vertical component recordings at different epicentral longitudes or two out of three components of recording at a single station. In practice we need 5 or 6 well-distributed stations to get well-constrained solutions and, even then, ambiguities will arise for certain kinds of events. A particular problem arises with "shallow" events ("shallow" being a relative term which is related to

the vertical wavelength of a mode). The fourth and fifth components of $g_i$ and $h_i$ are proportional to the $\epsilon_{r\theta}$ and $\epsilon_{r\phi}$ strains (cf. 4.34). These strains are related through the shear modulus to the horizontal tractions which are required to be zero at the free surface. We therefore anticipate that the fourth and fifth columns of $B_{ij}$ will be much smaller than the others for shallow events. This means that $\psi_4$ and $\psi_5$ do not contribute to the observed seismic energy for such events and so cannot be recovered. This is an important problem if we are interested in the source (e.g., its total moment) but is less important if we are only concerned with modeling the seismic data.

***Problem 4.2***

Assume that the source is a double-couple and is a shallow thrust event (slip angle = 270° ). Your procedure for estimation of $\psi$ gives you the solution with $||\psi||$ minimized. Explain why your answer has a dip angle of 45° and the smallest possible moment. If you know that the dip angle is about 20° , by how much should your estimate of moment be increased?

Usually when we fit for the moment tensor elements, we assume that the source is deviatoric and so apply the constraint that $M_{rr} + M_{\theta\theta} + M_{\phi\phi} = 0$. We can also apply a "plane constraint" if the source is a double-couple and the strike and dip of one plane is known (e.g., from a fault-plane solution).

We conclude this discussion of source retrieval by considering some of the reasons why solution of 4.50 may not allow us to fit the data as well as we would like. One obvious cause of misfit is noise. At low frequencies, small earthquakes are incapable of exciting large amplitudes and there will be little visible signal. We usually work in the 2–6 mHz band and find that we can successfully retrieve source mechanisms for events with moments greater than about $10^{26}$ dyne cm ($M_S \geq 6.5$). We find that the percentage variance reduction is independent of source size for events above $2 - 3 \times 10^{26}$ dyne cm so that the true noise is not the cause of misfit. The "noise" is actually scaling with the size of the event and so is "signal generated noise" – a euphemism for unmodeled signal. This unmodeled signal is mainly due to 3-D structure. You already know that apparent center frequencies of modes vary from great-circle to great-circle and will only occasionally agree with the frequency predicted by the model. Inspection of 4.50 shows that both $\mathbf{B}$ and $\mathbf{a}$ are "spikey." Schematically, we have

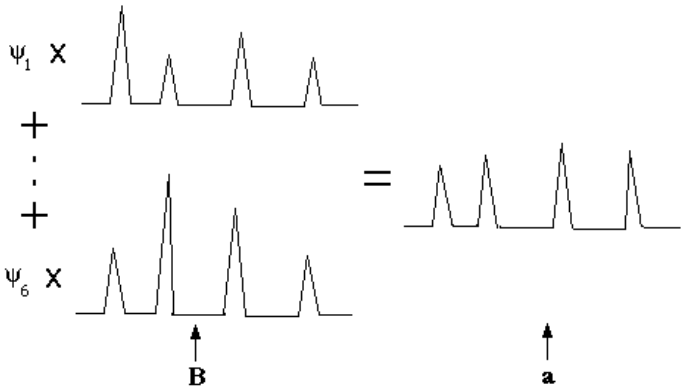


Given the fact that the spikes are not going to be perfectly aligned, we should expect that our solution will be biased to small moment (*i.e.*, we always end up fitting to the flanks of peaks). This is indeed the case and adjusting the solution to match the power in the data usually results in about a 10% increase in moment (source orientation seems to be relatively unaffected).

There are other sources of error. For the largest events, we expect that the effects of finite rupture and source mislocation will be important. These effects are very similar to the effects of 3-D structure and consequently it is difficult to see details of the rupture process. Better Greens functions computed for

good 3-D models will be required before details of the earthquake source can be divined from long-period data.

Even with spherical Earth Greens functions, we can often achieve a 70% variance reduction and produce imprecise synthetic seismograms (see Fig. 1, chapter 1). It appears to be true that all deep events ($\geq 400$ km) are extremely well fit while only about half the shallow events show good variance reductions. The reason for this remains obscure.

***4.7 Perturbation theory – spherical Earth .*** In this section we consider what happens when we perturb our Earth model. Eventually we shall consider the effect of a general perturbation but, for now, we shall restrict attention to perturbations which are spherically symmetric. In particular, the theory will allow us to compute the attenuation rate of a mode but it will also allow us to iteratively improve spherical Earth models to fit observations of mode frequencies.

We consider the effect of a perturbation in elastic properties and density. Our operator $\mathbf{L}$ becomes perturbed as does the displacement field and frequency, *i.e.*,

$$\begin{aligned}
\mathbf{L} &\to \mathbf{L} + \delta\mathbf{L} \\
\rho_0 &\to \rho_0 + \delta\rho_0 \\
\phi_0 &\to \phi_0 + \delta\phi_0 \\
\mathbf{s}_k &\to \mathbf{s}_k + \delta\mathbf{s}_k \\
\phi_{1k} &\to \phi_{1k} + \delta\phi_{1k} \\
\omega_k^2 &\to \omega_k^2 + \delta\omega_k^2
\end{aligned}$$

and our unperturbed solution satisfies equation 4.2:

$$\mathbf{L}(\mathbf{s}_k) + \rho_0\omega_k^2\mathbf{s}_k = 0$$

For now, we consider only perturbations such that the perturbed field satisfies all the boundary condition. Since $\mathbf{s}_k$ satisfies the boundary conditions, it follows that $\delta\mathbf{s}_k$ satisfies the boundary conditions and we use the result from section 3.9

$$-\omega_k^2 \int_V \rho_0 \mathbf{s}_k^\star \cdot \mathbf{s}_k \, dV = \int_V \mathbf{s}_k^\star \mathbf{L}(\mathbf{s}_k) \, dV \tag{4.53}$$

To first-order in the small perturbation we have

$$\begin{aligned}
-\omega_k^2 \int_V \rho_0 \mathbf{s}_k^\star \cdot \mathbf{s}_k \, dV - \delta\omega_k^2 \int_V \rho_0 \mathbf{s}_k^\star \cdot \mathbf{s}_k \, dV - \omega_k^2 \int_V \delta\rho_0 \mathbf{s}_k^\star \cdot \mathbf{s}_k \, dV \\
- \omega_k^2 \int_V \rho_0 \delta\mathbf{s}_k^\star \cdot \mathbf{s}_k \, dV - \omega_k^2 \int_V \rho_0 \mathbf{s}_k^\star \cdot \delta\mathbf{s}_k \, dV \\
= \int_V \mathbf{s}_k^\star \mathbf{L}(\mathbf{s}_k) \, dV + \int_V \mathbf{s}_k^\star \delta\mathbf{L}(\mathbf{s}_k) \, dV + \int_V \mathbf{s}_k^\star \mathbf{L}(\delta\mathbf{s}_k) \, dV + \int_V \delta\mathbf{s}_k^\star \mathbf{L}(\mathbf{s}_k) \, dV
\end{aligned} \tag{4.54}$$

Using 4.2, 4.53 and the self-adjointness of the operator $\mathbf{L}$, *i.e.*,

$$\int_V \mathbf{s}_k^\star \mathbf{L}(\delta\mathbf{s}_k) \, dV = \int_V \delta\mathbf{s}_k \mathbf{L}(\mathbf{s}_k^\star) \, dV$$

we end up with

$$\delta\omega_k^2 \int_V \rho_0 \mathbf{s}_k^\star \cdot \mathbf{s}_k \, dV = \int_V \mathbf{s}_k^\star \delta\mathbf{L}(\mathbf{s}_k) \, dV + \omega_k^2 \int_V \delta\rho_0 \mathbf{s}_k^\star \cdot \mathbf{s}_k \, dV \tag{4.55}$$

Equation 4.55 is our basic result. Note that it does not depend upon $\delta\mathbf{s}_k$ so, given $\delta\rho_0$, $\delta\mu$ and $\delta\kappa$ (so that $\delta\mathbf{L}$ may be computed) we can find $\delta\omega_k^2$. Equation 4.55 is not yet in a computationally useful form. We proceed by using the vector spherical harmonic representation of the displacement field of a toroidal or spheroidal mode:

$$\mathbf{s}_{k_{Toroidal}} = -\hat{\mathbf{r}} \times W \nabla_1 Y_l^m$$
$$\mathbf{s}_{k_{Spheroidal}} = \hat{\mathbf{r}} U Y_l^m + V \nabla_1 Y_l^m$$

where $U$, $V$ and $W$ are functions of radius for each mode. We can substitute these forms into equation 4.55 and perform the integrals over $\theta$ and $\phi$ analytically. Not surprisingly, we find that (for a spherical perturbation) the result is independent of the azimuthal order number, $m$. We are left with integrals over radius:

$$\delta\omega_k^2 \int_0^a \rho_0 N r^2 \, dr = \int_0^a \left[ K' \delta\kappa + M' \delta\mu + R\delta\rho_0 \right] r^2 \, dr \tag{4.56}$$

where, for spheroidal modes:

$$N = U^2 + l(l+1)V^2$$
$$K' = \left( \frac{dU}{dr} + F \right)^2$$
$$M' = \tfrac{1}{3} \left( 2\frac{dU}{dr} - F \right)^2 + \frac{l(l+1)}{r^2} \left( r\frac{dV}{dr} - V + U \right)^2 + \frac{1}{r^2}(l+2)(l-1)l(l+1)V^2$$
$$R = 2U \left( \frac{d\phi_1}{dr} + 4\pi G U \rho_0 - F\frac{d\phi_0}{dr} \right) + \frac{2}{r} V \phi_1 l(l+1) - \int_r^a 8\pi G \rho_0 U F \, dr - \omega_k^2 N$$

and, for toroidal modes:

$$N = l(l+1)W^2$$
$$K' = 0$$
$$M' = \frac{l(l+1)}{r^2} \left( r\frac{dW}{dr} - W \right)^2 + \frac{1}{r^2}(l+2)(l-1)l(l+1)W^2$$
$$R = -\omega_k^2 N$$

(Note that $d\phi_0/dr = g_0$). Equation 4.56 is our result but before we go on to use it, let us reconsider perturbation theory for the simple Sturm-Liouville problem that we set in section 3.7. This is already in terms of the radial eigenfunctions so we can derive the toroidal part of equation 4.56 very simply. We have

$$L(y) = (py')' - qy = -\lambda\tilde{\rho}y$$

where $y = W/r$, $p = \mu r^4$, $q = \mu r^2(l+2)(l-1)$, $\tilde{\rho} = \rho_0 r^4$, and $\lambda = \omega_k^2$. $L$ is self-adjoint, *i.e.*,

$$\int y_i L(y_j)\, dr = \int y_j L(y_i)\, dr$$

Now

$$\int_A^B yL(y)\, dr = \int_A^B y(py')'\, dr - \int_A^B qy^2\, dr = [ypy']_B^A - \int_A^B \left[p(y')^2 + qy^2\right]\, dr \tag{4.57}$$

Now $py'$ is proportional to the horizontal traction which must be zero at both boundaries for a mode solution. Thus 4.57 becomes

$$\int_A^B yL(y)\, dr = -\int_A^B \left[p(y')^2 + qy^2\right]\, dr = -\lambda \int_A^B \tilde{\rho} y^2\, dr \tag{4.58}$$

This we obtain on substitution of the original variables:

$$\omega_k^2 \int \rho_0 W^2 r^2\, dr = \int \left[\mu r^2 \left(\frac{dW}{dr} - \frac{W}{r}\right)^2 + \mu(l+2)(l-1)W^2\right]\, dr \tag{4.59}$$

Now from 4.55 we can write

$$-\delta\omega_k^2 \int \tilde{\rho} y_k^2\, dr = \int y_k \delta L(y_k)\, dr + \omega_k^2 \int \delta\tilde{\rho} y_k^2\, dr$$

$$\text{where} \quad \delta L(y_k) = (\delta p y_k')' - \delta q y_k$$

Hence

$$\int y_k \delta L(y_k)\, dr \equiv -\int [\delta p (y_k')^2 + \delta q y^2]\, dr$$

(we have assumed that the perturbed field matches the boundary conditions) and we get

$$\delta\omega_k^2 \int \tilde{\rho} y_k^2\, dr = \int [\delta p (y_k')^2 + \delta q y_k^2]\, dr - \omega_k^2 \int \delta\tilde{\rho} y_k^2\, dr \tag{4.60}$$

Equation 4.60 can now be converted to the usual form using the substitutions on the previous page, *i.e.*,

$$\delta\omega_k^2 \int \rho_0 r^2 W^2\, dr = \int \delta\mu \left[r^2 \left(\frac{dW}{dr} - \frac{W}{r}\right)^2 + (l+2)(l-1)W^2\right]\, dr - \omega_k^2 \int \delta\rho_0 r^2 W^2\, dr \tag{4.61}$$

If we multiply 4.61 through by $l(l+1)$ we get

$$\delta\omega_k^2 \int \rho_0 N r^2\, dr = \int [M'\delta\mu + R\delta\rho_0] r^2\, dr \tag{4.62}$$

where $N$, $M'$ and $R$ are defined as in 4.56.

***4.8 Attenuation .*** We now return to the problem of computing the attenuation rate of a mode. From section 4.6 we have perturbations of the form

$$\delta\mu = \frac{i\mu}{Q_\mu} \quad \text{and} \quad \delta\kappa = \frac{i\kappa}{Q_\kappa} \tag{4.63}$$

leading to a perturbation in $\omega_k^2$ given by

$$\frac{\delta\omega_k^2}{\omega_k^2} = \frac{i}{Q_k} \tag{4.64}$$

(this gives the attenuation rate of the mode $\alpha_k = \omega_k/2Q_k$). $Q_\mu$ and $Q_\kappa$ are functions of both depth and frequency and are a phenomenological description of dissipation processes. $Q_\mu$ gives the attenuation in shearing processes while $Q_\kappa$ gives the attenuation in compressional and dilatational processes. We assume that there is no imaginary part to the density ("imperfect inertia"?). Substitution of 4.63 and 4.64 into 4.56 gives

$$Q_k^{-1}\omega_k^2 \int_0^a \rho_0 N r^2\, dr = \int_0^a \left[\kappa K' Q_\kappa^{-1} + \mu M' Q_\mu^{-1}\right] r^2\, dr \tag{4.65}$$

Clearly, if we are given $Q_\mu^{-1}$ and $Q_\kappa^{-1}$, we can evaluate 4.65 to give $Q_k^{-1}$.

Careful consideration of 4.65 shows that $\kappa K'$ is proportional to the compressional energy density of the mode, $\mu M'$ is proportional to the shear energy density of the mode and $\omega_k^2\rho_0 N$ is proportional to the kinetic energy density of the mode. This is not surprising since $Q^{-1}$ is related to the fractional energy loss per cycle.

Equation 4.65 is also the basis for the inverse problem: given observations of $Q_k^{-1}$ for many modes, determine $Q_\kappa^{-1}(r,\omega)$ and $Q_\mu^{-1}(r,\omega)$. Of course, we need to know the elastic structure to calculate the energy densities in 4.65 but it is believed that the spherically averaged Earth structure is sufficiently well known that $\rho_0 N$, $\kappa K'$ and $\mu M'$ can be regarded as known for each mode. (There are a few exceptions to this, *i.e.*, modes which have turning points close to internal discontinuities can be extremely sensitive to structure in the vicinity of the turning point.) If we assume the energy densities are known, 4.65 is a *linear* inverse problem for $Q^{-1}$. If $Q_\mu^{-1}$ and $Q_\kappa^{-1}$ are doubled everywhere then $Q_k^{-1}$ is doubled. Linear inverse problems are well-studied and we shall consider this one in some detail. (For a full discussion of the $Q$ inversion problem see Masters and Gilbert, 1983 or Widmer at al, 1991 or Parker, 1994.)

The main problem we have in constraining $Q$ structure is that we have very few strictly independent constraints on the unknown model. A large proportion of the dataset is made up of $Q$ measurements for fundamental spheroidal modes. The energy distributions of these modes are dominated by shear energy in the upper mantle. Such modes are dominantly sensitive to $Q_\mu$ with depth sensitivity given by $\mu M' r^2$ in 4.65. We plot this for the modes ${}_0S_{21} \rightarrow {}_0S_{38}$ in figure 4.1. Note the extreme similarity of these functions and it is possible to construct any one of these functions from a linear combination of the seventeen others to about one part in a million. Clearly, if all eighteen of our data are to be independent constraints, the measurements must be extremely precise (to a part in a million!). Given the fact that the observations are good to a few percent, we know that our dataset has redundant data in it. One way of proceeding is to "rank and winnow" the data. To see how this is done we consider the simplest version of 4.65, *i.e.*,

$$\gamma_j \pm \sigma_j = \int_0^a g_j(r)\, m(r)\, dr \tag{4.66}$$

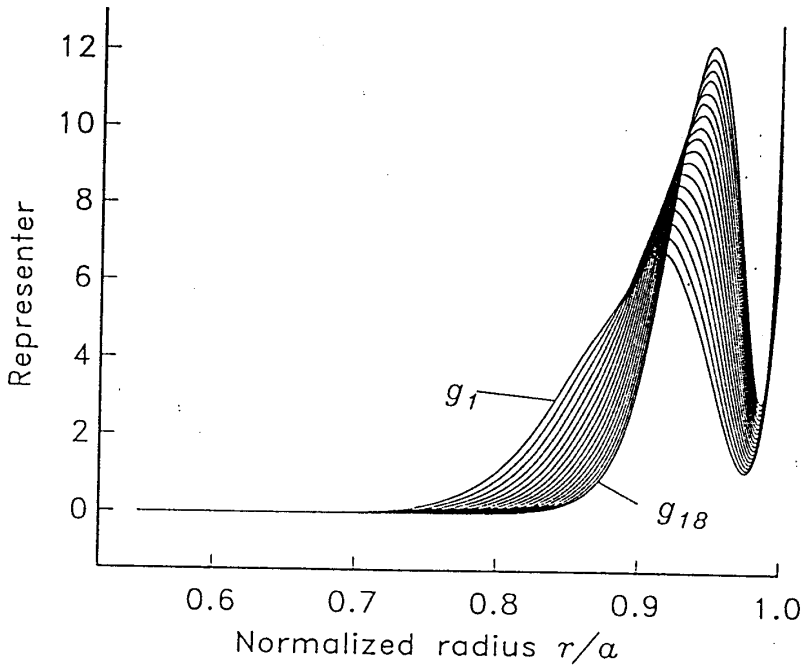


**Figure 4.1** $\mu M' r^2$ for ${}_0S_{21}, (g_1)$ to ${}_0S_{38}(g_{18})$. Note the extreme similarity of the kernels (sometimes called representers) to one another.

where $g_j$ is a data kernel or "representor" and $m(r)$ is our model.

We look for a recombination of our data, $\gamma_j$, which are orthogonal and precise. Our data will have a covariance matrix, $E_{ij}$, which is typically taken to be diagonal with elements $\sigma_i^2$, *i.e.*,

$$E_{ij} = \sigma_i^2 \delta_{ij} \tag{4.67}$$

First we divide 4.66 through by $\sigma_j$ to make the covariance matrix be the unit matrix, *i.e.*,

$$\frac{\gamma_i}{\sigma_i} \pm 1 = \int \frac{g_i(r)}{\sigma_i} m(r)\, dr = \int g_i'(r) m(r)\, dr = \gamma_i' \quad \text{say}$$

$$\text{and} \quad \mathbf{E}' = \mathbf{I} \tag{4.68}$$

Let the new data have representors which are linear combinations of the old representors with coefficients $\mathbf{B}$, *i.e.*,

$$\begin{aligned} \mathbf{B} \cdot \gamma' &= \int \mathbf{B} \cdot \mathbf{g}'(r)\, m(r)\, dr \\ \text{or} \quad \mathbf{d} &= \int \mathbf{G}(r)\, m(r)\, dr \end{aligned} \tag{4.69}$$

where $\mathbf{d} = \mathbf{B} \cdot \gamma'$, $\mathbf{G} = \mathbf{B} \cdot \mathbf{g}'$ and $\mathbf{B}$ is chosen so that the new data are orthogonal, *i.e.*,

$$\int G_i(r)G_j(r)\,dr = \delta_{ij}$$

$$\text{or} \quad \int \mathbf{G}\cdot\mathbf{G}^T\,dr = \mathbf{I}$$

$$\text{or} \quad \int \mathbf{B}\cdot\mathbf{g}'\cdot\mathbf{g}'^T\cdot\mathbf{B}^T\,dr = \mathbf{I}$$

$$\text{or} \quad \mathbf{B}\cdot\int \mathbf{g}'\cdot\mathbf{g}'^T\,dr\cdot\mathbf{B}^T = \mathbf{I}$$

or

$$\mathbf{B}\cdot\Gamma\cdot\mathbf{B}^T = \mathbf{I} \tag{4.70}$$

where

$$\Gamma = \int \mathbf{g}'\cdot\mathbf{g}'^T\,dr.$$

To find $\mathbf{B}$, we decompose $\Gamma$ into its eigenvalues and eigenvectors (it is a real, symmetric matrix so there are plenty of algorithms around for doing this):

$$\Gamma\cdot\mathbf{U} = \mathbf{U}\cdot\Lambda \tag{4.71}$$

where the columns of $\mathbf{U}$ are the eigenvectors and $\Lambda$ is the diagonal matrix of eigenvalues. Note that $\mathbf{U}^T\cdot\mathbf{U} = \mathbf{U}\cdot\mathbf{U}^T = \mathbf{I}$ so equation 4.70 can be written

$$\mathbf{I} = \mathbf{B}\mathbf{U}\Lambda\mathbf{U}^T\mathbf{B}^T \tag{4.72}$$

By inspection

$$\mathbf{B} = \Lambda^{-\frac{1}{2}}\,\mathbf{U}^T \tag{4.73}$$

and our new data, $\mathbf{B}\cdot\gamma' = \mathbf{d}$, have orthogonal kernels $\mathbf{G} = \mathbf{B}\cdot\mathbf{g}'$. The new data also have a covariance matrix given by

$$\mathbf{B}\cdot\mathbf{E}'\cdot\mathbf{B}^T = \mathbf{B}\cdot\mathbf{I}\cdot\mathbf{B}^T = \Lambda^{-1} \tag{4.74}$$

If we rank the eigenvalues and eigenvections of $\Gamma$ in order of decreasing magnitude, our first datum, $d_1$, will be the most precise and will have an error $\sqrt{1/\lambda_1}$. The second datum $d_2$, has error $1/\sqrt{\lambda_2}$ and so on. At some point, our new datum will be very imprecise so that we might truncate the dataset when $\sqrt{1/\lambda_n}$ exceeds some threshold value (this is called "winnowing"). Performing this procedure on the $Q$ dataset gives 29 combinations of the original data with errors of less than 50% and only 6 combinations of the original data with errors less than 10% – this is out of a total dataset of about 70 measurements.

Clearly, any attempt at model construction is going to require additional constraints to be able to say much about $Q$ structure inside the Earth. One solution we might pick (for no very good reason other than it is simple) is the solution with $\int m^2\,dr$ minimized. This is constructed in the following fashion. We have

$$\mathbf{d} = \int \mathbf{G}(r)\,m(r)\,dr$$

Let

$$m(r) = \sum \alpha_i G_i(r)$$

then

$$d_j = \sum \alpha_i \int G_i G_i \, dr = \sum \alpha_i \delta_{ij} = \alpha_j$$

Thus

$$m(r) = \sum d_i G_i(r) \tag{4.75}$$

Note that the coefficients in this expansion are just our new data and so become increasingly imprecise as $i$ increases. It is also almost always true that $G_i(r)$ become increasingly wiggly as $i$ increases, *i.e.*, the smoothest parts of the model are the most precisely determined. Other (more sensible) solutions requiring positivity and/or smoothness of $m(r)$ or that $m(r)$ is a monotonically decreasing or increasing function of depth are described in the papers cited above. Two models constructed with different smoothness criteria are shown in figure 4.2.

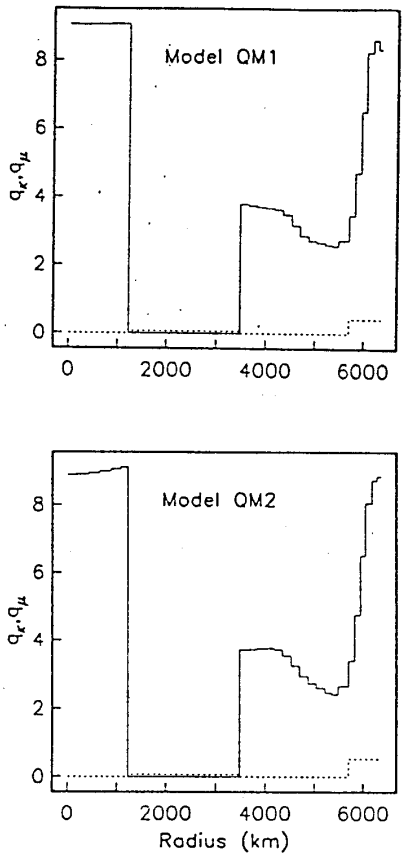


**Figure 4.2** Two smooth models which fit the $Q$ data. QM1 minimizes the sum of the first differences between layers and QM2 minimises the second differences. Note that $q \equiv 1000/Q$ and the dashed line is $q_K$ and the solid line is $q_\mu$.

We find that $Q$ decreases toward the surface of the Earth, *i.e.*, attenuation is more pronounced near the surface. The attenuation of the fundamental spheroidal modes can be explained simply in terms of the shear energy density becoming more concentrated towards the surface as $l$ increases. Thus the $Q$'s of the modes decrease as $l$ increases. Almost nothing can be said about frequency dependence of $Q$ from the mode dataset. The average $Q_\mu$ of the mantle (about 250) is very similar to the $Q$ inferred from the attenuation of $ScS$ body waves with periods of a few seconds. This is taken to be supportive of the assumption that $Q$ is roughly independent of frequency. We find the inner core to be extremely attenuating (in fact, more recent inversions have a $Q_\mu$ of about 70 in the inner core which is quite compatible with measurements of differential body-wave attenuation).

Equation 4.56 can also be used to improve the spherically averaged elastic structure of the Earth given estimates of the degenerate frequencies of multiplets. Before we look at this problem we first would like to extend 4.56 to include perturbations in the radii of internal discontinuities.

***4.9 Boundary perturbations .*** The variational principle we have been considering can be written in general as

$$\mathcal{L} = \int_V L \, dV \quad \text{and} \quad \delta\mathcal{L} = 0$$

where $L$ is a Lagrangian density and is a function of "fields", *i.e.*,

$$L = L(\mathbf{q}, \dot{\mathbf{q}}, m_i, \lambda)$$

where $m_i = \rho, \mu, \kappa$, etc, $\lambda = \omega_k^2$, and $\mathbf{q} = \mathbf{s}, \phi_1$, etc. For the variational principle to be satisfied $(\delta\mathcal{L} = 0)$ we must satisfy the Euler-Lagrange equations:

$$\left(\frac{\partial \dot{L}}{\partial \dot{\mathbf{q}}}\right) - \frac{\partial L}{\partial \mathbf{q}} = 0$$

with the boundary conditions

$$\left[\frac{\partial L}{\partial \dot{\mathbf{q}}}\right]_-^+ \cdot \hat{\mathbf{n}} = 0$$

Now suppose $m \to m + \delta m$ and suppose the perturbed problem also has $\delta\mathcal{L} = 0$ then the contribution from the perturbations in the field is zero to first order and we have

$$\int_V \left(\frac{\partial L}{\partial m_i}\delta m_i + \frac{\partial L}{\partial \lambda}\delta\lambda\right) dV = 0$$

or

$$\delta\lambda \int_V \frac{\partial L}{\partial \lambda} \, dV = -\int_V \frac{\partial L}{\partial m_i}\delta m_i \, dV$$

This is the equation that we have been using all along. Now suppose that this equation applies to the case of a perturbation in a boundary, $\delta h$. We would expect the answer to look like

$$\delta\lambda \int_V \frac{\partial L}{\partial \lambda} \, dV = \int_S [L]_-^+ \delta h \, dS$$

where $S$ is the surface, $\delta h$ is the normal displacement to the boundary and $[L]^+_-$ is the difference in the Lagrangian above and below the interface. This is the form that was originally used and is wrong.

The reason that this equation is wrong is that the perturbed fields do not satisfy the boundary condition and we must add another term to fix this up, *i.e.*,

$$\delta\lambda \int_V \frac{\partial L}{\partial \lambda}\, dV = \int_S \left[ L - \frac{\partial L}{\partial \dot{q}_i} \dot{q}_j n_i n_j \right]^+_- \delta h\, dS \tag{4.76}$$

As an example, consider the use of 4.76 when

$$L = \rho\omega^2 y^2 - \mu (y')^2$$

and there is a discontinuity in $\rho$ and $\mu$ at $h$ (this is almost the toroidal mode problem). The Euler-Lagrange equations give

$$(\mu y')' + \rho\omega^2 y = 0$$

and $\mu y'$ vanishes at the end points. Then 4.76 gives

$$\delta\omega^2 \int \rho y^2\, dx = \left[ L - \frac{\partial L}{\partial y'} y' \right]^+_- \delta h \tag{4.77}$$

but

$$\begin{aligned} L - \frac{\partial L}{\partial y'} y' &= \rho\omega^2 y^2 - \mu (y')^2 - (-2\mu y') y' \\ &= \rho\omega^2 y^2 + \mu (y')^2 \end{aligned}$$

Note that the incorrect expression would give $[\rho\omega^2 y^2 - \mu (y')^2]^+_- \delta h$ for the right hand side of 4.77 which, if $\rho$ is continuous at the interface, has precisely the wrong sign!

To proceed in the general case, we consider the perturbation to the equations of motion when a boundary is perturbed and use the boundary conditions to calculate the perturbations in the fields $\delta\mathbf{s}$, $\delta\phi_1$ and $\delta\mathbf{T}$ which are required to keep the boundary conditions satisfied. For example, consider a welded boundary. Now

$$[\mathbf{s} + \delta\mathbf{s}]^{h+\delta h^+}_{h+\delta h^-} = 0$$

where $h + \delta h$ is the radius of the perturbed discontinuity. Expand $\mathbf{s}$ in a Taylor series so

$$\mathbf{s}(h + \delta h) = \mathbf{s}(h) + \delta h \partial_r \mathbf{s}(h) + \cdots$$

therefore

$$[\mathbf{s} + \delta h \partial_r \mathbf{s} + \delta\mathbf{s}]^{h^+}_{h^-} = 0$$

or

$$\delta\mathbf{s} = -\delta h [\partial_r \mathbf{s}]^+_- \tag{4.78}$$

Thus we can calculate $\delta\mathbf{s}$ in terms of the perturbation in the boundary and the radial derivative of the unperturbed eigenfunctions. In this way we can eliminate all references to the unknown perturbations in $\mathbf{s}$ and replace them with terms proportional to $\delta h$. A complete list of substitutions is:

$$
\begin{aligned}
[\delta \mathbf{s}] &= -\delta h [\partial_r \mathbf{s}]^+_- && \text{welded} \\
[\delta s_r] &= -\delta h [\partial_r s_r]^+_- && \text{fluid/solid} \\
[\delta \mathbf{T} \cdot \hat{\mathbf{r}}] &= -\delta h [\delta_r \mathbf{T} \cdot \hat{\mathbf{r}}]^+_- && \text{all} \\
[\delta \phi_1] &= -\delta h [\partial_r \phi_1]^+_- && \text{all} \\
[\partial_r \delta\phi_1 + 4\pi G \rho_0 \delta s_r] &= -\delta h [\partial_r (\partial_r \phi_1 + 4\pi G \rho_0 s_r)]^+_- && \text{all}
\end{aligned}
\tag{4.79}
$$

where all terms on the right are evaluated at the unperturbed boundary. One other complication arises because moving a discontinuity causes a perturbation in $\rho_0$, $\mu$, $\kappa$ in $h \to h + \delta h$ but $\phi_0$ is perturbed everywhere. In effect, a shell of density $[\rho]^+_-$ of thickness $\delta h$ is added so

$$
\left.
\begin{aligned}
\delta\phi_0 &= \frac{4\pi G h^2}{r} [\rho]^+_- \delta h \quad \text{for} \quad r > b \\
&= \text{constant} \quad \text{for} \quad 0 < r < b
\end{aligned}
\right\}
\tag{4.80}
$$

We now go through the perturbation theory using 4.79 and 4.80 to eliminate the field perturbations. The result is

$$
\begin{aligned}
\delta\omega^2 \int \rho_0 \mathbf{s}^* \cdot \mathbf{s}\, dV = & \int_V \rho_0 \left[ \mathbf{s} \cdot \mathbf{s}^* \nabla(\nabla \delta\phi_0) + \nabla\delta\phi_0 (\mathbf{s}^* \cdot (\nabla \mathbf{s})^T - \mathbf{s}^* \cdot (\nabla \cdot \mathbf{s})] \right. \, dV \\
& - \delta h \int_S [\nabla \mathbf{s}^* \cdot\cdot \mathbf{C} : \nabla \mathbf{s} + \rho_0 (\mathbf{s}^* \cdot \nabla \phi_1 + \mathbf{s} \cdot \nabla \phi_1^* + \mathbf{s} \cdot \mathbf{s}^* \nabla(\nabla \phi_0)) \\
& - \nabla\phi_0 ((\mathbf{s}^* \cdot (\nabla \mathbf{s})^T - \mathbf{s}^* (\nabla \cdot \mathbf{s})) - \omega^2 \mathbf{s} \cdot \mathbf{s}^*) \\
& + \frac{1}{4\pi G} \nabla\phi_1 \cdot \nabla\phi_1^* - \hat{\mathbf{r}} \cdot [\nabla \mathbf{s}^* \cdot\cdot \mathbf{C} : \nabla \mathbf{s} + \nabla \mathbf{s} \cdot\cdot \mathbf{C} : \nabla \mathbf{s}^* \\
& + \left. \nabla\phi_1 \cdot (\frac{1}{4\pi G} \nabla\phi_1^* + \rho_0 \mathbf{s}^*) + \nabla\phi_1^* (\frac{1}{4\pi G} \nabla\phi_1 + \rho_0 \mathbf{s})] \right]^+_- \cdot \hat{\mathbf{r}}\, dS
\end{aligned}
\tag{4.81}
$$

This rather complicated equation can be cast in a form suitable for computation using the usual vector spherical harmonics. The result is

$$
\delta\omega^2 \int_0^a \rho_0 N r^2\, dr = -\delta h [\kappa K'' + \mu M'' + \rho_0 R]^+_- \tag{4.82}
$$

where

$$
\begin{aligned}
K'' &= F^2 - (\partial_r U)^2 \\
M'' &= \tfrac{1}{3} [F^2 - (2\partial_r U)^2] + \frac{l(l+1)}{r^2} [(U - V)^2 - (r\partial_r V)^2 + W^2 - (r\partial_r W)^2] \\
&\quad + \frac{1}{r^2} [l(l+1) - 2] l(l+1) [V^2 + W^2]
\end{aligned}
\tag{4.83}
$$

$N, R$ are defined in equation 4.56. Equation 4.82 allows us to compute the perturbation in a mode frequency when a boundary is moved by $\delta h$. We can combine 4.82 and 4.56 to give the starting point for the inverse problem for spherically averaged structure:

$$\frac{\delta\omega}{\omega} = \int \left( K\frac{\delta\kappa}{\kappa} + M\frac{\delta\mu}{\mu} + R\frac{\delta\rho}{\rho} \right) dr + \sum_k A_k \delta h_k \tag{4.84}$$

where $K$, $M$, $R$ and $A_k$ can be computed for each mode given a starting model and $\delta\omega$ can be interpreted as $\omega_{observed} - \omega_{model}$. Equation 4.84 is a *linearized* inverse problem and must be solved iteratively, *i.e.*, at each iteration we find new $\delta\kappa$, $\delta\mu$, $\delta\rho$, $\delta h_k$ which (partially) fit the $\delta\omega$'s then $K$, $M$, $R$ and $A_k$ are recomputed for the perturbed model. If we have enough observations of modes of different kinds (e.g., $PKIKP$ equivalent, $ScS$ equivalent etc), $K$, $M$, $R$ and $A_k$ will be significantly different functions of depth for each mode and we will be able to learn about the details of Earth structure. In practice, the success of this procedure is entirely dependent upon the quality of the estimates of the degenerate eigenfrequencies and bias in the observations is common.

***4.10 Estimating degenerate eigenfrequencies .*** An important result which we shall prove in chapter 5 is the "diagonal sum rule." Any aspherical perturbation will cause a multiplet to be split but the diagonal sum rule states that, to first order in small quantities, the sum of the singlet frequencies is just the degenerate frequency of the multiplet. This is often taken to mean that, if we measure the center frequency of a split multiplet for a good geographical distribution of source-receiver pairs, the average frequency will be the frequency of the spherically averaged Earth. There are some hidden assumptions in this statement which we shall look at later. Where do degenerate frequency estimates come from? Measurements of peak frequencies from single recordings can provide good degenerate frequency estimates for highly excited, isolated multiplets. Such frequency measurements form simple geographic patterns when viewed as a function of the pole of the great circle joining the source and receiver and the mean of this pattern can be shown to be a good estimate of the degenerate frequency (see later chapters). Unfortunately, this analysis is confined to a small subset of modes – mainly the fundamental spheroidal modes. These modes do not sample the deep Earth and are incapable of giving us high resolution estimates of Earth structure. For this, we require overtone measurements and to obtain overtone measurements we have to use multiple-record data analysis techniques. We consider two techniques – "stacking" and "stripping." Reconsider 4.35:

$$\mathbf{s}(\mathbf{r}, \mathbf{r}_0, t) = \sum_{n,l} \sum_{i=1}^{6} {}_n\mathbf{G}_l^i(\mathbf{r}, \mathbf{r}_0) \psi_i(t) \star \frac{1}{{}_n\omega_l^2} {}_nC_l(t)$$

$$\text{where} \quad {}_nC_l(t) = [1 - \cos({}_n\omega_l t) e^{-{}_n\alpha_l t}] H(t)$$

This equation tells us that, as $t \to \infty$, we get a nonzero static offset. In practice, we remove the mean from the recording so the static offset is removed. Suppose we have made an estimate of $\psi(t)$ and let the $n, l$'th mode be denoted by $k$ and let a single component of recording for the $\mathbf{r}, \mathbf{r}_0$ source-receiver pair be denoted by $j$. Define

$$B_{jk} = -\frac{1}{\omega_k^2} \sum_{i=1}^{6} {}_kG_j^i \psi_i(t)$$

$$C_k(t) = \cos(\omega_k t) e^{-\alpha_k t} H(t)$$

then 4.35 becomes

$$s_j(t) = \sum_k B_{jk}(t) \star C_k(t) \tag{4.85}$$

Note that $\psi(t)$ is usually close to being a $\delta$ function in time so that $B_{jk}$ will be a slowly varying function of frequency. In fact, we may take $B_{jk}$ to be independent of frequency in a small frequency band which encompasses several modes of interest. Equation (4.85) becomes

$$s_j(\omega) = \sum_k B_{jk}(\omega) C_k(\omega) \simeq \sum_k B_{jk} C_k(\omega) \tag{4.86}$$

Remember that we taper the data when we take the FFT so 4.86 can be regarded as an inverse problem to recover tapered resonance function, $C_k(\omega)$, if $B_{jk}$ can be computed. We assume that we have a good enough Earth model and source mechanism so that a reasonable estimate of $B_{jk}$ can be made. Equation 4.86 can be rewritten:

$$\mathbf{s}(\omega) = \mathbf{B} \cdot \mathbf{C}(\omega)$$

Stacking is

$$\mathbf{s}'(\omega) = \mathbf{B}^T \cdot \mathbf{s}(\omega) = \mathbf{B}^T \cdot \mathbf{B} \cdot \mathbf{C}(\omega) \tag{4.87}$$

Stripping is

$$\mathbf{s}''(\omega) = \mathbf{B}^{-1} \cdot \mathbf{s}(\omega) = \mathbf{B}^{-1} \cdot \mathbf{B} \cdot \mathbf{C}(\omega) \tag{4.88}$$

Consider stacking first. A multiplet consists of singlets of the form

$$\mathbf{s} = U\mathbf{A}_l^m + V\mathbf{B}_l^m + W\mathbf{C}_l^m$$

where

$$\mathbf{A}_l^m = \hat{\mathbf{r}} Y_l^m, \quad \mathbf{B}_l^m = \nabla_1 Y_l^m \quad \text{and} \quad \mathbf{C}_l^m = -\hat{\mathbf{r}} \times \nabla_1 Y_l^m$$

Inspection of 4.33 shows that $\mathbf{B}$ has a similar form. Now

$$\int \mathbf{A}_l^{m*} \cdot \mathbf{A}_{l'}^{m'} \, d\Omega = \int \mathbf{B}_l^{m*} \cdot \mathbf{B}_{l'}^{m'} \, d\Omega = \int \mathbf{C}_l^{m*} \cdot \mathbf{C}_{l'}^{m'} \, d\Omega = 0$$

unless $l = l'$ and $m = m'$. Similarly all cross products of $\mathbf{A}$'s, $\mathbf{B}$'s and $\mathbf{C}$'s are zero. Now suppose that we have a dense set of source-receiver pairs which are globally distributed. The matrix product $\mathbf{B}^T \cdot \mathbf{B}$ then tends to a surface integral and becomes diagonally dominant. Thus $\mathbf{s}'$ becomes proportional to $\mathbf{C}$ and, performing the operation 4.87 at each frequency, gives us an estimate of the spectrum of each multiplet resonance function.

Stripping is a little more straightforward. We simply form a generalized inverse of $\mathbf{B}$ so that $\mathbf{s}''$ should give a direct estimate of $\mathbf{C}$. Since $\mathbf{B}$ is independent of frequency, we need only form its inverse once and and then apply it to each frequency in turn. The advantage of stripping is that it only requires as many records as modes in the band (in principle) and so usually works better than stacking. On the other hand, stacking is usually less sensitive to errors in source mechanisms, etc. An example of stripping is given in Figure 1.14. The center frequency and attenuation rate of each multiplet can now be estimated from their stacks and strips and can be used as data in the inverse problem for spherically averaged structure. Care should be taken to avoid bias from the signal due to aspherical structure. In particular, both stacking and stripping assume that there is an even distribution of singlets within a multiplet. Clearly, if the singlets are clumped to one end of a multiplet, adding up many records will tend to give a peak at that end of the multiplet and will not give a peak at the degenerate frequency. Usually, when this happens the strips have multiple peaks (see example of ${}_1S_4$ in figure 4.3) and so the problem can be diagnosed.

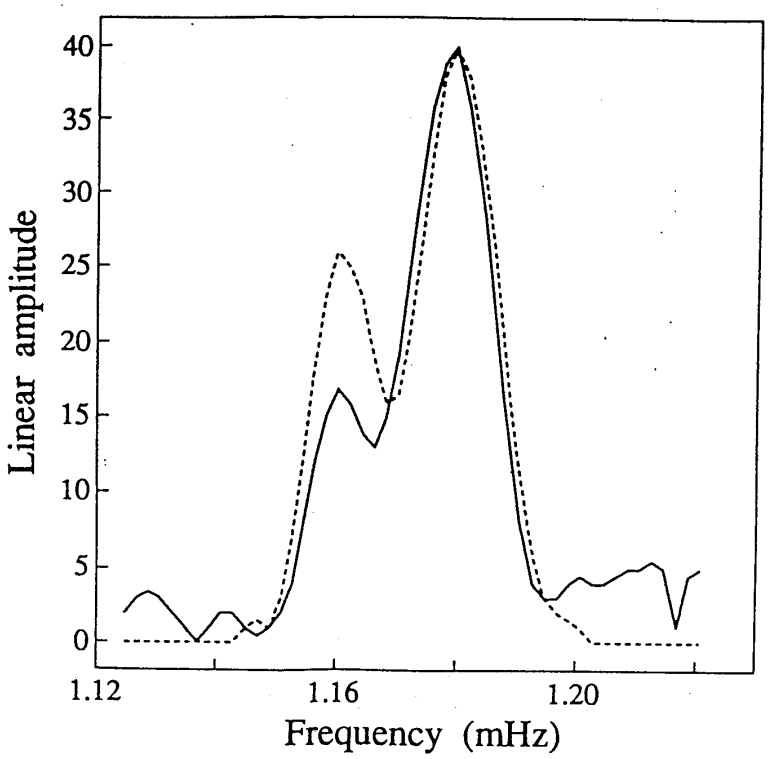


**Figure 4.3** A multiplet strip for ${}_1S_4$. The solid line is a strip of data and the dashed line is a strip of synthetic data. This demonstrates that multiplet stripping is incapable of giving good degenerate frequencies for broadly split multiplets with a non-uniform distribution of singlets.

Occasionally one obtains a clear single-peak strip at the extreme end of a multiplet which, if interpreted as the degenerate frequency, introduces bias into the dataset.

For most high $l$ ($l \geq 10$) multiplets, the distribution of singlets within a multiplet is sufficiently uniform that stacking or stripping with a good geographical distribution of source-receiver pairs gives strips with peaks close to the degenerate frequencies. Figures 4.4 and 4.5 show strips for ${}_0S_l$ and ${}_0T_l$ modes and the center frequencies of the ${}_0S_l$ modes measured from the strips can be compared with those obtained from the analysis of individual recordings (Fig. 4.6). The agreement is good but both datasets show unusual jumps in the $\omega/l$ curve (Figure 4.6). As we shall see later, such jumps are caused by coupling to toroidal modes and the frequencies again should not be interpreted as belonging to isolated spheroidal modes. The cause of this coupling is dominantly the Coriolis force and so can be modeled. We can estimate the mean shift of a hybrid multiplet's frequency from the uncoupled degenerate value and correct the data so that it can be used to constrain the spherically averaged structure.

For modes which cannot be analyzed by multiplet stacking and stripping or by a single record analysis, we must model the split spectra directly or try and isolate each singlet within the multiplet. The degenerate frequency can then be estimated by invoking the diagonal sum rule. Modes which must be analyzed in this fashion are the low $l$, high $Q$ multiplets which sample into the core (see Ritzwoller *et al.,* 1986, 1988). The occurrence of the recent Bolivian event has resulted in many new accurate degenerate frequencies for such modes.

Currently we have about 900 reliable degenerate frequency estimates which are being analyzed for spherically averaged structure. The ability of this mode dataset to constrain structure are discussed in

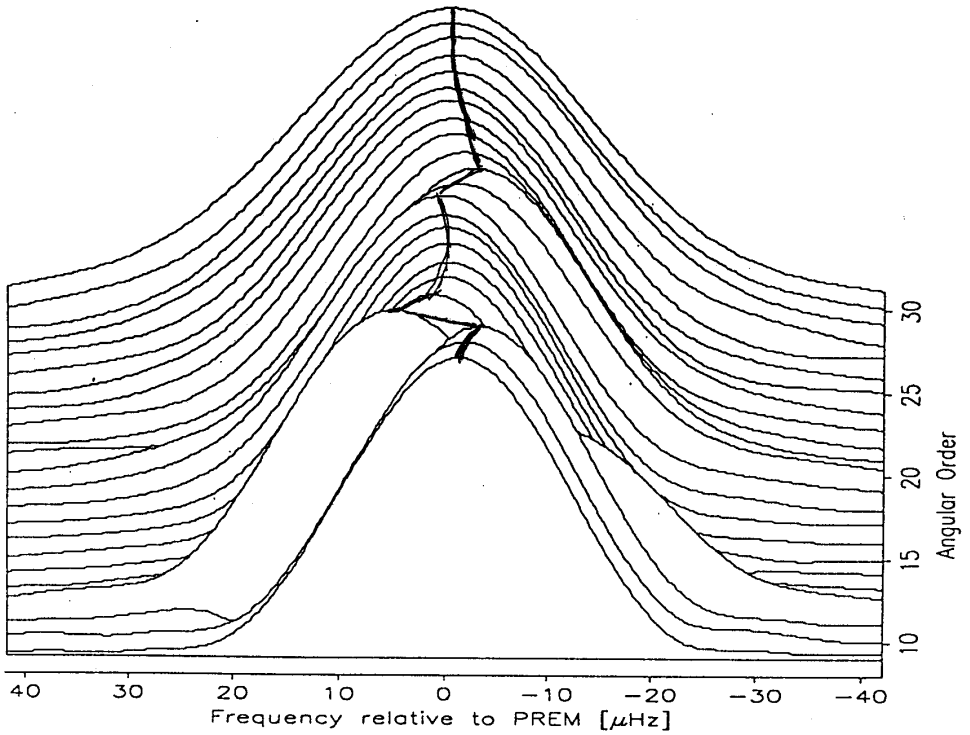


**Figure 4.4** The results of stripping fundamental spheroidal modes ${}_0S_8$ to ${}_0S_{30}$. the strips are centered at the frequency predicted by each mode for PREM. Note the "tears" in the peak shifts caused by Coriolis coupling to nearby toroidal modes.

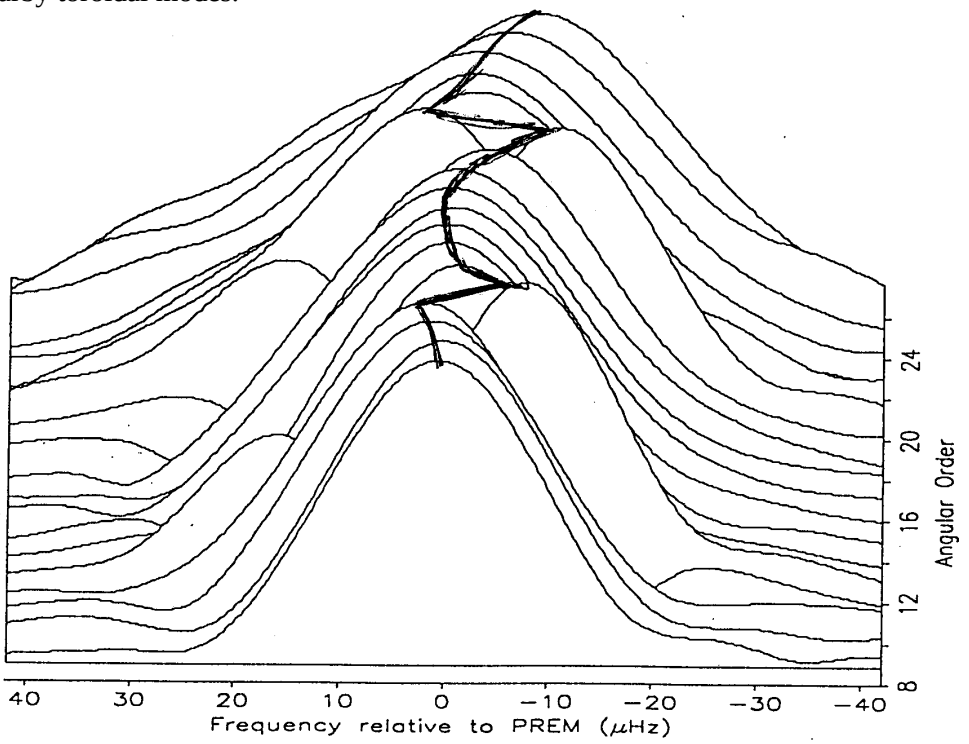


**Figure 4.5** As for figure 4.4 but for toroidal modes ${}_0T_8$ to ${}_0T_{26}$.

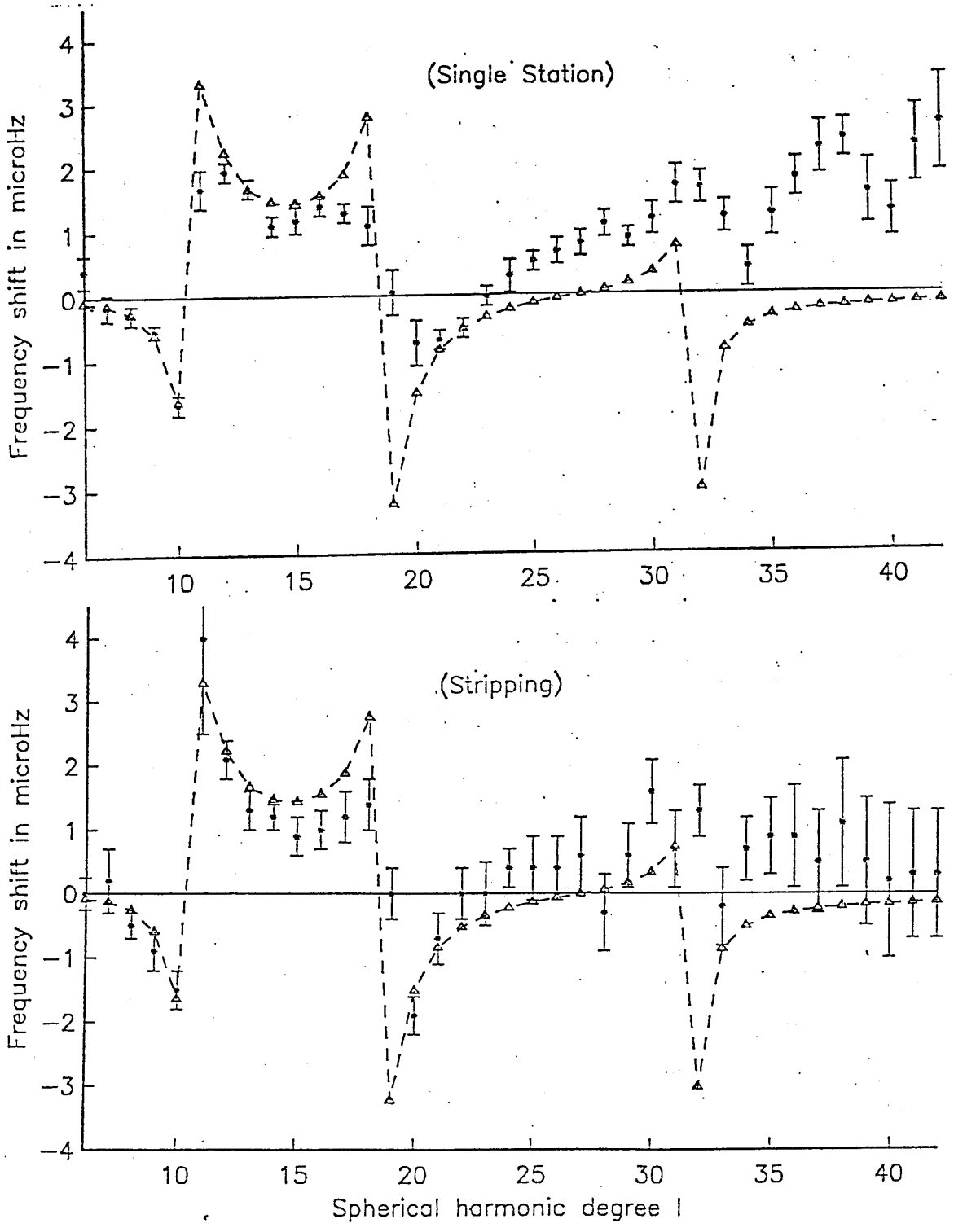


**Figure 4.6** Fundamental spheroidal mode peak frequencies plotted relative to those of model 1066A obtained by (top) looking at peak shifting patterns from single record analyses and (bottom) by using the multiplet stripping technique. The triangels are estimates of the theoretical peak shift due to Coriolis coupling (see chapter 5).

the reprint on ”resolution”.

Some general conclusions:

1) If allowed, small amounts of transverse isotropy ($\approx 0.2\%$) throughout the solid regions of the Earth. This is in contrast to PREM which has about 2% in the top 200 km. In fact, there is a strong trade-off between the depth at which anisotropy is allowed to extend and the size of discontinuities in the upper mantle (e.g. Montagner and Anderson, 1989). The jump in shear velocity at the 410 km discontinuity tends to disappear if significant anisotropy is allowed to extend below about 200 km.
2) Models with sharp upper-mantle discontinuities fit the data better than smooth upper-mantle models. Sharp discontinuities cause a measurable “solotone effect” in some overtone sequences – particularly the ${}_nS_0$ radial modes.
3) Modes which sample strongly near the core-mantle boundary tend to be poorly fit suggesting that we might not have a correct parameterization of structure here. Allowing sharp discontinuities just above or below the core-mantle boundary gives a modest improvement in fit to these data.

Continued improvement of spherically averaged models will require careful attention to biases in the degenerate frequency data set since quality, rather than quantity, is what is required to give good resolution of Earth structure.

***Problem 4.3***

In body-wave seismology, the concept of a spherically averaged Earth may not seem very useful. Why does this same concept make sense for mode seismology?